Institut für Numerische Simulation
Rheinische Friedrich-Wilhelms-Universität Bonn
Wegelerstraße 6 • 53115 Bonn • Germany
phone +49 228 73-3427 • fax +49 228 73-7527
www.ins.uni-bonn.de

D. L. Brown, D. Peterseim

Localization of Multiscale Problems with Porous Microstructures

INS Preprint No. 1410

November 2014

A Multiscale Method for Porous Microstructures

Donald L. Brown* Daniel Peterseim†

July 10, 2015

Abstract

In this paper we develop a multiscale method to solve problems in complicated porous microstructures with Neumann boundary conditions. By using a coarse-grid quasi-interpolation operator to define a fine detail space and local orthogonal decomposition, we construct multiscale corrections to coarse-grid basis functions with microstructure. By truncating the corrector functions we are able to make a computationally efficient scheme. Error results and analysis are presented. A key component of this analysis is the investigation of the Poincaré and inverse inequality constants in perforated domains as they may contain micro-structural information. Using first a theoretical method based on extensions of functions and then constructive method originally developed for weighted Poincaré inequalities, we are able to obtain estimates on Poincaré constants with respect to scale and separation length of the pores. Finally, two numerical examples are presented to verify our estimates.

1 Introduction

Modeling and simulation of porous media has many wide ranging applications in engineering. For example, to simulate heat or electric conductivity in complicated materials or composites a partial differential equation (PDE) in complicated microstructures must be solved. Direct numerical simulation of such problems is difficult, and, in some scenarios is intractable. The main challenge being the many scale nature of the problem and complex geometries involved. In these applications, where there are many scales and complex heterogeneities, numerical homogenization procedures are employed to reduce complexity yet remain accurate. In this work, we develop a multiscale method to simulate Neumann problems in domains with porous microstructures.

The study of multiscale problems in porous or perforated domains has a long history. In the area of homogenization of partial differential equations, there is a vast literature on the subject [8, 23, 28] and references therein, to name just a few. In these problems, the fine-scale equations have microstructure, then through an averaging process of homogenization an effective PDE is derived. In these methods, the strong assumption of periodicity is usually made, and thus, only one microstructure dependent local problem is solved to compute effective properties. The coarse-grid, or homogenized problem, does not have explicit microstructure. More computationally based procedures have also been investigated. Using an approach based on the Heterogeneous Multiscale Method [2], an algorithm was developed in [15] by solving for an unknown diffusion coefficient on the coarse-grid by resolving a local perforated domain problem. Then, computation on the coarse-grid equation is based in an effective non-porous domain. Further work, [6], developed a perforated multiscale finite element method for Dirichlet problems utilizing Crouzeix-Raviart non-conforming finite elements. Using the MsFEM framework [9], a weak Crouzeix-Raviart boundary condition is used to construct the multiscale finite element basis that include the vanishing Dirchlet condition into the basis functions. There are also mesoscopic schemes that relax the resolution condition of standard finite elements insofar as they allow that mesh cells are cut by the domain boundary; see e.g. [4, 5, 10, 11, 19] among many

*Institute for Numerical Simulation, University of Bonn, brown@ins.uni-bonn.de
†Institute for Numerical Simulation, University of Bonn

others. However, for those schemes there are typically strong restrictions on the topology of the intersection that rule out the case of perforation on the element level.

We will work in the multiscale framework using a local orthogonal decomposition (LOD) [22], which is inspired by the variational multiscale method [18, 17, 20]. For a general introduction and discussion we refer the reader to [26]. The LOD method uses a coarse-grid quasi-interpolation operator to decompose the space into fine-scale components to build the fine detail space. From the fine detail space we are able to build multiscale corrections to the coarse-grid functions and construct a multiscale space. These corrections have global support, thus limiting their practical usage. However, these corrections have fast decay and can therefore be localized. This procedure has been used effectively for elliptic problems with L^∞ coefficients [13, 16, 22], been extended to semi-linear elliptic equations [14], linear and nonlinear eigenvalue problems [12, 21], and to the wave equation [1].

In this work, we extend this framework to the case when we have microstructures that generate the multiscale features as opposed to oscillatory and highly varying coefficients. We first build a coarse-perforated grid, then by using a quasi-interpolation operator based on local L^2 projection build a fine-scale space. We again follow the process in [13, 16, 22] of multiscale space construction, localization, and subsequent error estimates. We show that we can obtain the same error estimates with respect to coarse-grid size and truncation of local problems as in these works. However, in this setting we are particularly concerned with the tracking of Poincaré constants in perforated domains as these may depend on the micro-structural features, namely the size of particles and separation length. Using the methods developed in [25], originally for the setting of high-contrast coefficients and weighted Poincaré inequalities, we are able to create a constructive procedure to estimate these constants in domains with microstructure. This is carried out for a few interesting examples. We show that in the case of a reticulated filamented structure it is possible that the microstructural features can negatively impact this Poincaré constant in the case of very thin structures. In addition, we show that in the case of isolated particles we obtain uniform (microstructure independent) Poincaré constants.

The paper is organized as follows. We begin by the problem setting and the description of quasi-interpolations in perforated domains. This quasi-interpolation will allow us to construct our multiscale orthogonal splitting and subsequent computational localization algorithm. Then, we will derive error estimates on both global supported and localized basis functions. This is done with the help of technical lemmas in the Appendix and careful tracking of relevant constants. We then develop a constructive procedure to estimate Poincaré constants in porous domains. Finally, we give two numerical examples to demonstrate the rates of convergence with respect to mesh parameters, localization truncation, and microstructure lengths. In addition, we discuss overall effectiveness of the algorithm and the choices of possible quasi-interpolation operators.

2 Problem Set Up

We now begin with some notation and problem setting. Let $\Omega \subset \mathbb{R}^d$ be a bounded Lipschitz domain with polyhedral boundary for $d \geq 2$. We denote the solid microstructure to be $\{S_i\}_{i=1}^N$, a set of Lipschitz nonintersecting closed subsets of Ω. We denote the perforated domain, often called fluid or porous domain, $\widetilde{\Omega} = \Omega \backslash \mathcal{S}$, where $\mathcal{S} = \cup_{i=1}^N S_i$. We supposed that the solid microstructure or inclusions are so that $\widetilde{\Omega}$ remains connected and Lipschitz. We let η be the characteristic size of the microstructure. Moreover, we let η also be the minimal separation length. These two parameters may be considered separately, but for clarity we choose them to be on the same order of magnitude. We suppose for simplicity that the perforations do not intersect the global boundary, but may be η close to it. An example geometry can be seen in Figure 1.

We wish to find a solution u that satisfies

$$-\Delta u = g \text{ in } \widetilde{\Omega}, \tag{1a}$$

$$\frac{\partial u}{\partial n} = 0 \text{ on } \partial\mathcal{S}, \tag{1b}$$

$$u = 0 \text{ on } \partial\Omega. \tag{1c}$$

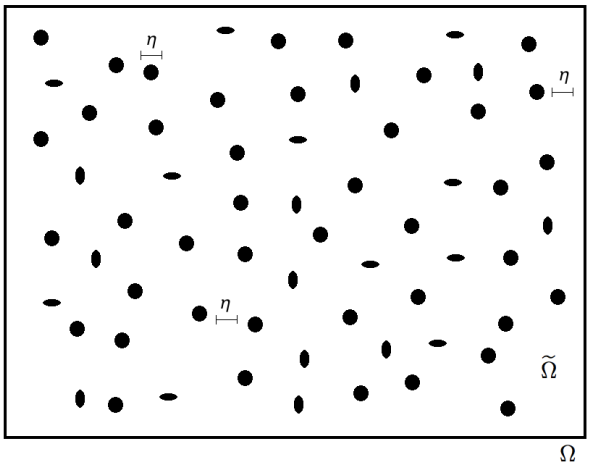

Figure 1: Domain Ω with microstructure. The porous part of the domain is denoted $\widetilde{\Omega}$.

Where $g \in L^2(\widetilde{\Omega})$, and n denotes the outer normal on $\partial\mathcal{S}$.

We denote the space $H^1_D(\widetilde{\Omega}) := \{v \in H^1(\widetilde{\Omega}) \mid v = 0 \text{ on } \partial\widetilde{\Omega}\}$. Multiplying by $v \in H^1_D(\widetilde{\Omega})$ and integrating (1), we wish to solve for $u \in H^1_D(\widetilde{\Omega})$ such that

$$\int_{\widetilde{\Omega}} \nabla u \nabla v dz = \int_{\widetilde{\Omega}} g v dz, \tag{2}$$

here dz is the standard real Lebesgue measure in $\mathbb{R}^d$. The main difficulty in solving the above problem is the mutliscale nature introduced from the microstructure. We may also add in an oscillatory coefficient inside the perforated domain $\widetilde{\Omega}$, however, this case is well studied in [22] and we focus on the issues involved with the multiscale geometries.

3 Quasi-Interpolation in Perforated Domains

In this section we develop the framework to work on perforated domains. We first define the classical nodal basis restricted to $\widetilde{\Omega}$ the perforated domain. Then, we describe how to construct a quasi-interpolation that is also projective, in contrast to the quasi-interpolation operator used in [22].

3.1 Classical Nodal Basis

Following much of the notation in [22], suppose that we have a coarse quasi-uniform discretization $\mathcal{T}_H$ of the unperforated domain Ω with mesh size H. We denote the interior nodes not on the boundary of the coarse mesh as $\mathcal{N}_H$. Let the classical conforming $\mathbb{P}_1$ finite element space over $\mathcal{T}_H$ be given by S_H, and let $V_H = S_H \cap H^1_0(\Omega)$. We denote the nodal basis functions λ_y, that is for an interior node $y \in \mathcal{N}_H$, we have

$$\lambda_x(x) = 1 \text{ and } \lambda_y(x) = 0, y \neq x. \tag{3}$$

This is a basis for V_H. Let $u_H \in V_H$ be the function satisfying

$$\int_{\Omega} \nabla u_H \nabla v dz = \int_{\Omega} g v dz, \text{ for all } v \in V_H.$$

To move to the perforated domain it is useful to have some more notation. We denote the restriction operator of a function on Ω to $\widetilde{\Omega}$ by $\mathcal{R} : H^1_0(\Omega) \to H^1_0(\widetilde{\Omega})$. We denote the space of finite element functions

(3) restricted to the perforated domain as

$$\widetilde{V}_H = \{w| \text{ there exists } u \in V_H, w = \mathcal{R}u\} = \mathcal{R}\widetilde{V}_H.$$

From here we may define a coarse-grid variational form of (2). Indeed, let $\tilde{u}_H \in \widetilde{V}_H$ be the function satisfying

$$\int_{\widetilde{\Omega}} \nabla \tilde{u}_H \nabla v dz = \int_{\widetilde{\Omega}} g v dz, \text{ for all } v \in \widetilde{V}_H. \tag{4}$$

However, $\tilde{u}_H$ will not be a good approximation to $\tilde{u}$ unless H is sufficiently small to resolve the microstructure.

3.2 Projective Quasi-Interpolation

In this section, we develop the theory for a quasi-interpolation operator that is also a projection. This projective quasi-interpolation gives stability properties required for the localization theory without the use of an auxiliary "closeness to projection" lemma used in the theory of Clément quasi-interpolation theory c.f. Lemma 1 of [13]. This requires the construction of a function that satisfies certain interpolation properties and derivative bounds. However, in the case of perforated domains such a construction can be quite tedious and an alternate approach is utilized here.

We will construct a quasi-interpolation operator that is also projective and satisfies the requisite local stability properties. For non-perforated domains, this is a modification of the operator of Clément [24]. We denote the local patch $\text{supp}(\lambda_x) = \omega_x$ for $x \in \mathcal{N}_H$ and, subsequently, the perforated patch as $\widetilde{\omega}_x = \omega_x \cap \widetilde{\Omega}$. First, we define the local patch L^2 projection $\mathcal{P}_x : L^2(\widetilde{\omega}_x) \to V_H|_{\omega_x}$, as the operator such that for $u \in H^1_D(\widetilde{\omega}_x)$

$$\int_{\widetilde{\omega}_x} (\mathcal{P}_x u) v_H dz = \int_{\widetilde{\omega}_x} u v_H dz \text{ for all } v_H \in V_H|_{\omega_x} \tag{5}$$

From this we define the interpolation operator $\widetilde{\mathcal{I}}_H : H^1_D(\widetilde{\Omega}) \to \widetilde{V}_H$ for $u \in H^1_D(\widetilde{\Omega})$ as

$$\widetilde{\mathcal{I}}_H u = \sum_{y \in \mathcal{N}_H} (\mathcal{P}_y u)(y) \mathcal{R}\lambda_y(x). \tag{6}$$

Given a function $\phi \in H^1_D(\widetilde{\Omega})$ with support contained in a patch of triangles $\widetilde{\omega}_x$, then, by the definition of the quasi-interpolation (6), it is clear that $\text{supp}(\widetilde{\mathcal{I}}_H(\phi)) \not\subset \widetilde{\omega}_x$ in general, as the boundary nodes on the patch $\widetilde{\omega}_x$ will add a contribution smearing out the function. To deal with this issue we require some notation and definitions. Using the definition and notation in [13], we define for any patch ω_x the extension patch

$$\omega_x = \omega_{x,0} = \text{supp}(\lambda_x) \cap \Omega, \tag{7a}$$

$$\omega_{x,k} = \text{int}(\cup\{T \in T_H | T \cap \widetilde{\omega}_{k-1} \neq \emptyset\} \cap \Omega, \tag{7b}$$

for $k = 1, 2, 3, 4, \ldots$, and denote $\{\widetilde{\omega}_{x,k}\}_{k \in \mathbb{N}}$ to be the corresponding perforated domains. With this notation we have $\text{supp}(\widetilde{\mathcal{I}}_H(\phi)) \subset \overline{\widetilde{\omega}}_{x,1}$ if $\text{supp}(\phi) \subset \widetilde{\omega}_{x,0}$ for the interpolator (6).

Remark Further with some slight more notation. Throughout this entire work, we will use the symbol $A \lesssim B$ to mean $A \leq CB$, where $C > 0$ and is independent of microstructure parameters and coarse grid size H.

It will be important to note that we have a Poincaré constant in the estimate below. Since our domain can have complicated microstructure we must be careful when analyzing estimates that contain this constant. We suppose that we have the following general Poincaré inequality for each patch $\widetilde{\omega}_x$ for $x \in \mathcal{N}_H$. Moreover, we shall suppose that this constant serves as a global bound with respect to H and η. The analysis of such a constant will be considered in Section 6.

We recall the Poincaré inequality here. For all $\widetilde{\omega}_x$ with $x \in \mathcal{N}_H$, we have for $\phi \in H^1(\widetilde{\Omega})$

$$\left\|\phi - \bar{\phi}\right\|_{L^2(\widetilde{\omega}_x)} \leq H C_P^x(\eta, H) \left\|\nabla \phi\right\|_{L^2(\widetilde{\omega}_x)}, \tag{8}$$

Where $C_P^x(\eta, H)$ may depend on the diameter of the triangulation, and subsequently ω_x, and its characteristic microstructure parameter η. We denote $C_P(\eta, H) = \max_{x\in\mathcal{N}_H} C_P^x(\eta, H)$ and will drop the notation (η, H) in many of the estimates throughout the paper when there is no ambiguity.

In addition, the finite element inverse inequality on perforated domains contains a volumetric constant that also must be tracked throughout. This constant is further analyzed and discussed in Appendix A. In particular, we have the general result Lemma 3.1. It can be seen here that this constant behaves like ϕ^{-1}, where ϕ is the porosity or volume fraction. Thus, we expect this constant to interfere with our estimates in the case where the domain is very perforated. We state this inequality briefly here.

Lemma 3.1 *Let $K \in \mathcal{T}_H$ be a simplex in $\mathbb{R}^d$ and $p \in \mathbb{P}_1(K)$. Let $\tilde{K} \subset K$ be a finite union of polygons, then*

$$\|\nabla p\|_{L^2(\tilde{K})} \lesssim \left(\frac{|K|}{|\tilde{K}|}\right) H^{-1} \|p\|_{L^2(\tilde{K})}, \tag{9}$$

We will denote

$$C^{inv} = \max_{K\in\mathcal{T}_H, \tilde{K}\subset K} \left(\frac{|K|}{|\tilde{K}|}\right),$$

and track this constant throughout the analysis.

Proof See Appendix A.

We have the following stability and local approximation of the quasi-interpolation operator $\widetilde{\mathcal{I}}_H$ defined by (6), along with the desired projective properties.

Lemma 3.2 *There exists a constant $C_{\mathcal{I}_{H,1}}, C_{\mathcal{I}_{H,2}} > 0$, for all $u \in H_D^1(\widetilde{\Omega})$, such that*

$$\left\|u - \widetilde{\mathcal{I}}_H u\right\|_{L^2(\widetilde{\omega}_{x,0})} \leq C_{\mathcal{I}_{H,1}} H \|\nabla u\|_{L^2(\widetilde{\omega}_{x,1})}, \tag{10a}$$

$$\left\|\nabla(u - \widetilde{\mathcal{I}}_H u)\right\|_{L^2(\widetilde{\omega}_{x,0})} \leq C_{\mathcal{I}_{H,2}} \|\nabla u\|_{L^2(\widetilde{\omega}_{x,1})}, \tag{10b}$$

where $C_{\mathcal{I}_{H,1}} \lesssim (1 + C^{inv})C_P$ and $C_{\mathcal{I}_{H,2}} \lesssim \big(1 + (1 + C^{inv})C_P\big)$. We denote $C_{\mathcal{I}_H}$ to be

$$\max(C_{\mathcal{I}_{H,1}}, C_{\mathcal{I}_{H,2}}) \lesssim C_{\mathcal{I}_H} \lesssim C^{inv} C_P.$$

Here C_P is the Poincaré constant and C^{inv} the finite element inverse inequality constant in perforated domains. Moreover, the interpolation $\widetilde{\mathcal{I}}_H$ is a projection.

Proof See Appendix B.

4 Multiscale Splitting and Basis

We now will construct our multiscale approximation space to handle the oscillations created by the perforated microstructure. The main ideas of this splitting can be found in [13, 22] and references therein. As noted before the coarse mesh space restricted to $\widetilde{\Omega}$ can not resolve the features of the microstructure and these fine-scale features must be captured in the multiscale basis. We begin by constructing fine-scale spaces.

We define the kernel of the perforated interpolation operator to be

$$\widetilde{V}^f = \{v \in H_D^1(\widetilde{\Omega}) \mid \widetilde{\mathcal{I}}_H v = 0\},$$

where $\widetilde{\mathcal{I}}_H$ is defined by (6). This space will represent the small scale features not captured by $\widetilde{V}_H$. We define the fine-scale projection $Q_{\widetilde{\Omega}} : \widetilde{V}_H \to \widetilde{V}^f$ to be the operator such that for $v \in \widetilde{V}_H$ we compute $Q_{\widetilde{\Omega}}(v) \in \widetilde{V}^f$ as

$$\int_{\widetilde{\Omega}} \nabla Q_{\widetilde{\Omega}}(v) \nabla w dz = \int_{\widetilde{\Omega}} \nabla v \nabla w dz, \text{ for all } w \in \widetilde{V}^f. \tag{11}$$

This projection gives an orthogonal splitting $H^1_D(\widetilde{\Omega}) = \widetilde{V}^{ms}_H \oplus \widetilde{V}^f$ with $\widetilde{V}^{ms}_H = (\widetilde{V}_H - Q_{\widetilde{\Omega}}(\widetilde{V}_H))$. We can decompose any $u \in H^1_D(\widetilde{\Omega})$ as $u = u^{ms} + u^f$ with $\int_{\widetilde{\Omega}} \nabla u^{ms} \nabla u^f dz = 0$. This modified coarse space is referred to as the multiscale space and contains fine-scale geometric information. The multiscale Galerkin approximation $u^{ms}_H \in \widetilde{V}^{ms}_H$ satisfies

$$\int_{\widetilde{\Omega}} \nabla u^{ms}_H \nabla v dz = \int_{\widetilde{\Omega}} g v dz \text{ for all } w \in \widetilde{V}^{ms}_H. \tag{12}$$

To construct the basis for the multiscale space $\widetilde{V}^{ms}_H$ we construct an adapted coarse grid basis. We define the corrector $\phi_x = Q_{\widetilde{\Omega}}(\lambda_x)$ to be the solution to

$$\int_{\widetilde{\Omega}} \nabla \phi_x \nabla w dz = \int_{\widetilde{\Omega}} \nabla \lambda_x \nabla w dz, \text{ for all } w \in \widetilde{V}^f. \tag{13}$$

We then define the perforated multiscale space $\widetilde{V}^{ms}_H$ to be the functions spanned by

$$\widetilde{V}^{ms}_H = \text{span}\{\mathcal{R}\lambda_x - \phi_x | x \in \mathcal{N}_H\}. \tag{14}$$

Note that the corrector problem (11) is posed on the global domain. Thus, the corrections will have global support and as such have limited practical use. However, in the following analysis we show that the basis can be localized.

The key issue with constructing the solution to (12) is the calculation of the corrector on a global basis. However, it can be shown that the corrector decays exponentially fast. To this end, we define the localized fine-scale space to be the fine-scale space extended by zero outside the patch, that is $\widetilde{V}^f(\widetilde{\omega}_{x,k}) = \{v \in \widetilde{V}^f |\ v|_{\widetilde{\Omega}\setminus\widetilde{\omega}_{x,k}} = 0\}$. It is convenient to introduce some notion here similar to that introduced in [13]. We let for some $x \in \mathcal{N}_H$ and $k \in \mathbb{N}$ the local corrector operator $Q_{x,k} : \widetilde{V}_H \to \widetilde{V}^f(\widetilde{\omega}_{x,k})$, be defined such that given a $u_H \in \widetilde{V}_H$

$$\int_{\widetilde{\omega}_{x,k}} \nabla Q_{x,k}(u_H) \nabla w dz = \int_{\widetilde{\omega}_x} \hat{\lambda}_x \nabla u_H \nabla w dz, \text{ for all } w \in \widetilde{V}^f(\widetilde{\omega}_{x,k}), \tag{15}$$

where $\hat{\lambda}_x = \frac{\lambda_x}{\sum_{y\in\mathcal{N}_H} \lambda_y}$ is augmented so that the collection $\{\hat{\lambda}_x\}_{x\in\mathcal{N}_H}$ is a partition of unity. This is done because the Dirchlet condition makes the standard basis not a partition of unity near the boundary. For a practical evaluation of $Q_{x,k}$, we may precompute for any neighbor $y \in \mathcal{N}_H \cap \widetilde{\omega}_x$ of x the following

$$\int_{\widetilde{\omega}_{x,k}} \nabla Q_{x,k}(\lambda_y) \nabla w dz = \int_{\widetilde{\omega}_x} \hat{\lambda}_x \nabla \lambda_y \nabla w dz, \text{ for all } w \in \widetilde{V}^f(\widetilde{\omega}_{x,k}). \tag{16}$$

We then write $Q_{x,k}(u_H) = \sum_{y\in\mathcal{N}_H\cap\widetilde{\omega}_x} u_H(y) Q_{x,k}(\lambda_y)$ and so must only compute over small number of nearby nodes for each x. Moreover, we are able to exploit local periodic structures due to the fact that a drastically reduced number of corrector problems must be computed, assuming the coarse-grid is chosen properly.

We denote the global corrector operator as

$$Q_k(u_H) = \sum_{x\in\mathcal{N}_H} Q_{x,k}(u_H).$$

With this notation, we write the truncated multiscale space as

$$\widetilde{V}^{ms}_{H,k} = \text{span}\{u_H - Q_k(u_H) | u_H \in \widetilde{V}_H\}.$$

Moreover, note also that for sufficiently large k, we recover the full domain and obtain the ideal corrector with functions of global support, denoted $Q_{\widetilde{\Omega}}$. The corresponding multiscale approximation to (2) is

$$\int_{\widetilde{\Omega}} \nabla u^{ms}_{H,k} \nabla v dz = \int_{\widetilde{\Omega}} g v dz \text{ for all } w \in \widetilde{V}^{ms}_{H,k}. \tag{17}$$

5 Error Analysis

In this section we present the error introduced by using (12) on the global domain to compute the solution to (2). Then, we show how localization effects the error when we use (17) on truncated domains to compute the same solution. Meanwhile, we must carefully account for the effects of the Poincaré constant from (8) in the estimate as in certain domains this may depend on the microstructure or coarse grid diameters.

5.1 Error with Global Support

Theorem 5.1 *Suppose that $u \in H^1_D(\widetilde{\Omega})$ satisfies* (2) *and that $u_H^{ms} \in \widetilde{V}_H^{ms}$, with correctors of global support in* (13)*, satisfies* (12)*. Then, we have the following error estimate*

$$\|\nabla u - \nabla u_H^{ms}\|_{L^2(\widetilde{\Omega})} \leq C_{\mathcal{I}_{H,1}} H \|g\|_{L^2(\widetilde{\Omega})}. \tag{18}$$

Proof Again we use the local stability property of $\widetilde{\mathcal{I}}_H$ the local interpolation operator in (10). From the orthogonal splitting of the spaces it is clear that $u - u_H^{ms} = u^f \in \widetilde{V}^f$ and $\widetilde{\mathcal{I}}_H(u^f) = 0$. Thus, using the stability inequality we have

$$\|\nabla u - \nabla u_H^{ms}\|^2_{L^2(\widetilde{\Omega})} = \left\|\nabla u^f\right\|^2_{L^2(\widetilde{\Omega})} = \int_{\widetilde{\Omega}} g\left(u^f - \widetilde{\mathcal{I}}_H(u^f)\right) dz$$
$$\|g\|_{L^2(\widetilde{\Omega})}\left\|u^f - \widetilde{\mathcal{I}}_H(u^f)\right\|_{L^2(\widetilde{\Omega})} \leq C_{\mathcal{I}_{H,1}} H \|g\|_{L^2(\widetilde{\Omega})}\left\|\nabla u^f\right\|_{L^2(\widetilde{\Omega})}$$

Taking $u^f = u - u_H^{ms}$ and dividing, we arrive at the estimate (18). □

5.2 Error with Localization

In this section we show the error due to truncation with respect to patch extensions. The key lemma needed is the following estimate, the proof can be found in Appendix C.

Lemma 5.2 *Let $u_H \in \widetilde{V}_H$, let Q_m be constructed from* (15)*, and $Q_{\widetilde{\Omega}}$ defined to be the "ideal" corrector without truncation, then*

$$\left\|\nabla(Q_{\widetilde{\Omega}}(u_H) - Q_m(u_H))\right\|_{L^2(\widetilde{\Omega})} \leq m^{\frac{d}{2}} C_4 \theta^m \left\|\nabla Q_{\widetilde{\Omega}}(u_H)\right\|_{L^2(\widetilde{\Omega})}, \tag{19}$$

with $\theta \in (0,1)$, $C_3 \lesssim (1 + C_1 + C_{\mathcal{I}_H}) \lesssim (C^{inv}C_P)^{3/2}$ and $C_4 = C_3(1 + C_1^2)^{\frac{1}{2}} \lesssim (C^{inv}C_P)^3$.

The lemma gives the decay in the error as the truncated corrector approaches the ideal corrector of global support. With this lemma we are able to state and prove Theorem 5.3.

Theorem 5.3 *Suppose that $u \in H^1_D(\widetilde{\Omega})$ satisfies* (2) *and that $u_{H,m}^{ms} \in \widetilde{V}_{H,m}^{ms}$, with local correctors calculated from* (15)*, satisfies* (17)*. Then, we have the following error estimate*

$$\left\|\nabla u - \nabla u_{H,m}^{ms}\right\|_{L^2(\widetilde{\Omega})} \leq \left(C_{\mathcal{I}_{H,1}} H + m^{\frac{d}{2}} C_5 \theta^m\right) \|g\|_{L^2(\widetilde{\Omega})}, \tag{20}$$

with $\theta \in (0,1)$ a constant depending on Poincaré and inverse inequality constants. In addition, with respect to these constants we have

$$C_{\mathcal{I}_{H,1}} \lesssim C^{inv}C_P, \text{ and } C_5 \lesssim C_P^4 (C^{inv})^3.$$

Remark Note from Lemma C.2, we have $\theta = e^{-\frac{1}{\lceil C_2 e \rceil + 2}} \in (0,1)$, here $C_2 = (C_1 + CC_{\mathcal{I}_H}) \lesssim (C^{inv}C_P)^{3/2}$. Thus, the Poincaré and inverse constants effect the estimate in Lemma C.2 insofar as it may slower the decay rate of the exponential and not lead to some sort of exponential "blow-up" with respect to patch extensions.

Proof of Theorem 5.3 We let $u_H^{ms} = u_H - Q_{\widetilde{\Omega}}(u_H)$ be the ideal global multiscale solution satisfying (12), and $u_{H,m}^{ms} = u_{H,m} - Q_m(u_{H,m})$ the corresponding truncated solution to (17). Then, by Galerkin approximations being minimal in energy norm we have

$$\|\nabla u - \nabla(u_{H,m} - Q_m(u_{H,m}))\|_{L^2(\widetilde{\Omega})} \lesssim \|\nabla u - \nabla(u_H - Q_m(u_H))\|_{L^2(\widetilde{\Omega})}.$$

Using this fact and Theorem 5.1 and Lemma C.3 we have

$$\begin{aligned}
\left\|\nabla u - \nabla u_{H,m}^{ms}\right\|_{L^2(\widetilde{\Omega})} &\leq \left\|\nabla u - \nabla(u_H - Q_{\widetilde{\Omega}}(u_H) + Q_{\widetilde{\Omega}}(u_H) - Q_m(u_H))\right\|_{L^2(\widetilde{\Omega})} \\
&\leq \|\nabla u - \nabla u_H^{ms}\|_{L^2(\widetilde{\Omega})} + \left\|\nabla(Q_{\widetilde{\Omega}}(u_H) - Q_m(u_H))\right\|_{L^2(\widetilde{\Omega})} \\
&\leq C_{\mathcal{I}_{H,1}} H \|g\|_{L^2(\widetilde{\Omega})} + \left\|\nabla(Q_{\widetilde{\Omega}}(u_H) - Q_m(u_H))\right\|_{L^2(\widetilde{\Omega})} \\
&\leq C_{\mathcal{I}_{H,1}} H \|g\|_{L^2(\widetilde{\Omega})} + m^{\frac{d}{2}} C_4 \theta^m \left\|\nabla Q_{\widetilde{\Omega}}(u_H)\right\|_{L^2(\widetilde{\Omega})}.
\end{aligned}$$

Finally, noting that from (15) and (12) we have

$$\left\|\nabla Q_{\widetilde{\Omega}}(u_H)\right\|_{L^2(\widetilde{\Omega})} \leq \|\nabla u_H^{ms}\|_{L^2(\widetilde{\Omega})} \leq C_P \|g\|_{L^2(\widetilde{\Omega})},$$

applying this above we obtain the required estimate.

To obtain the relationship on the above estimate to the relevant constants note from (10) that $C_{\mathcal{I}_H} \lesssim C^{inv} C_P$. From Lemma C.1, we have $C_1^2 = C_{lip}^2 C_{\mathcal{I}_H} + C_{\mathcal{I}_H}^3$, thus $C_1 \lesssim (C^{inv} C_P)^{\frac{3}{2}}$. From Lemma C.3,

$$C_4 = C_3(1 + C_1^2)^{\frac{1}{2}} = (1 + C_1 + C_{\mathcal{I}_H})(1 + C_1^2)^{\frac{1}{2}} \lesssim (C^{inv} C_P)^3,$$

and so $C_5 = C_P C_4 \lesssim C_P^4 (C^{inv})^3$. □

6 Estimates for Poincaré Constants

In this section, we discuss the tools required to estimate the constant C_P in certain physically interesting cases. We will give two alternative approaches. The first is the case where the particles are of size $\eta > 0$ and have minimal separation from each other and the boundary also of order $\eta > 0$. This is accomplished by using extension approaches that preserve the Sobolev seminorm [7] and we will primarily use a slightly more modern presentation as in [30]. This more theoretical approach works very well for isolated particles and proves to be a powerful tool in estimating these constants.

In addition, we will also consider a constructive approach that could be extended to the case where there are high contrast coefficients inside the domain and can be used when the particles are not isolated in a simple way. The following techniques were developed and used effectively in the context of weighted Poincaré inequalities in the setting of contrast dependence [25] and references therein. We follow much of the notation presented in that work, however, here we adapt the techniques to complex domain geometries and not contrast independent estimates. The case of high-contrast for non-perforated domains will be discussed in the forthcoming preprint [27].

We begin by building the necessary framework to effectively estimate C_P by a theoretical extension approach. Then, we present a constructive approach by building the some what complicated machinery for weighted Poincaré inequalities. Throughout this section we shall suppose that $H > \eta$, the characteristic separation and length scale size.

6.1 Poincaré Constants: Extension Techniques

In this section, we will show that estimates for isolated particles in two-dimensions can be shown to be uniformly bounded. The key ingredient of this is utilizing a construction of the Stein-Whitney extension [31] for domains with small isolated particles and showing that the related constants do not contain microstructural information.

We will now outline how such an extension is constructed. We suppose that as in [7, 30, 29], that the maximal diameter of the isolated particles is η and this is also the minimal separation length from each of the particles and the boundary. To be more precise, we suppose that we have non intersecting subsets $S_1, S_2, \cdots, S_N \subset \omega$ (removing the x label for this section), such that $\text{diam}(S_j) := \eta_j \lesssim \eta$, for $j = 1, 2, \ldots N$, and naturally define

$$\widetilde{\omega} = \omega \backslash \bigcup_{j=1}^{N} \bar{S}_j$$

We suppose that each S_j can be enclosed by a shape regular polygonal U_j, and its homothetic expansion V_j, for $j = 1, 2, \ldots N$, such that

$$\begin{aligned} &S_j \subset U_j \subset V_j \subset \omega, \\ &V_j \cap V_i = \emptyset, \text{ for } i \neq j, \\ &\Delta_i := V_j \backslash \bar{U}_j, \text{ is simply connected.} \end{aligned} \tag{21}$$

Remark Note that the boundaries above can be taken to just be minimally smooth in the sense of Stein [31] as seen in [30, 29]. However, assuming that they can be enclosed in shape regular polygons is enough for our applications.

Further we assume that the boundaries are properly separated for that there exists constants $C_1, C_2 > 0$ such that

$$C_1 \eta_j \leq \text{dist}(\partial V_j, \partial S_j) \leq C_2 \eta_j, \tag{22}$$

for $j = 1, 2, \ldots N$. We denote the Stein extension operator on Δ_i to be $E_i : H^1(\Delta_i) \to H^1(\mathbb{R}^d)$, such that $E_i u = u$ on Δ_i and $|E_i u|_{H^1(\mathbb{R}^d)} \lesssim |u|_{H^1(\Delta_i)}$, [7]. We then take the extension of $u \in H^1(\widetilde{\omega})$ to ω to be defined as

$$u^{ext} = \begin{cases} E(u|_{\Delta_i}) \text{ in } U_i, \\ u \text{ elsewhere in } \omega. \end{cases}$$

Then, it is shown in [30, 29] that

$$\left\| u^{ext} \right\|_{H^1(\omega)} \lesssim C_{ext} \left\| u \right\|_{H^1(\widetilde{\omega})}, \tag{23}$$

where C_{ext} depends only on $\text{diam}(\omega)$ and is independent of the diameter and separation of the holes. Thus, we see that

$$\begin{aligned} \left\| u - \langle u^{ext} \rangle_\omega \right\|_{L^2(\widetilde{\omega})} &\leq \left\| u - u^{ext} \right\|_{L^2(\widetilde{\omega})} + \left\| u^{ext} - \langle u^{ext} \rangle_\omega \right\|_{L^2(\widetilde{\omega})} \\ &\leq \sum_{j=1}^{N} \left\| u - u^{ext} \right\|_{L^2(U_j \backslash S_j)} + \left\| u^{ext} - \langle u^{ext} \rangle_\omega \right\|_{L^2(\omega)} \\ &\leq C_{FP} \max_{j=1}^{N} (\text{diam}(U_j)) \sum_{j=1}^{N} |u - u^{ext}|_{H^1(U_j \backslash S_j)} + \left\| u^{ext} - \langle u^{ext} \rangle_\omega \right\|_{L^2(\omega)}, \end{aligned}$$

where C_{FP} is a Frederich's type constant since $u - u^{ext}$ vanishes on the boundaries of ∂U_j, and this constant is known to be an advantageous constant with respect to perforations. Using a global Poincaré inequality, independent of the holes, on the second term and the extension estimate (23) we obtain using the minimality of the average that

$$\left\| u - \langle u \rangle_{\widetilde{\omega}} \right\|_{L^2(\widetilde{\omega})} \leq \left\| u - \langle u^{ext} \rangle_\omega \right\|_{L^2(\widetilde{\omega})} \lesssim \text{diam}(\widetilde{\omega}) \left\| u \right\|_{H^1(\widetilde{\omega})}, \tag{24}$$

or that $C_P \lesssim 1$ and is independent of η. Finally, applying this estimate to Theorem 5.3 we have

$$\left\| \nabla u - \nabla u^{ms}_{H,m} \right\|_{L^2(\widetilde{\Omega})} \leq \left(C^{inv} H + m^{\frac{d}{2}} (C^{inv})^3 \theta^m \right) \left\| g \right\|_{L^2(\widetilde{\Omega})}. \tag{25}$$

Recall here that from Appendix A, the constant C^{inv} depends only volumetrically on the microstructure and under the separation assumptions, will not contribute very much error and one can suppose that order one.

6.2 Poincaré Constants: Constructive Approach

Now that we have given a theoretical extension approach for domains with isolated and regularly separated particles, we will outline a constructive approach that may have wider applicability at the cost of complexity and elegance of the proof. This constructive approach is used in [25] in the context of high-contrast elliptic problems, whereby the Poincaré inequalities are weighted so that they do not depend on the contrast. This approach may have wider applicability in problems of the form

$$-\text{div}(A\nabla u) = f \text{ in } \widetilde{\Omega},$$

where $A \in L^\infty$ and $\alpha \leq |A| \leq \beta$, for $\alpha, \beta > 0$ and β/α is very large.

We begin by examining a domain $\widetilde{\omega}$ (removing the x as above) that is assumed in this section to be partitionable into non overlapping polytopes. In essence, the perforations must be (or approximated by) polygons. Further, we begin as in [25], let $\mathcal{Y} = \{Y_l\}_{l=1}^n$ be a non overlapping partitioning of $\widetilde{\omega}$ into open, connected Lipschitz polytopes so that

$$\overline{\widetilde{\omega}} = \bigcup_{l=1}^{n} \overline{Y}_l,$$

with $H = \text{diam}(\omega)$. For $u \in H^1(\widetilde{\omega})$ and $(d-1)$ dimensional manifold $X \subset \widetilde{\omega}$ we define the average

$$\bar{u}^X = \frac{1}{|X|}\int_X u ds,$$

here the above integral is taken with respect to the $(d-1)$ dimensional real Lebesgue measure ds.

We call a region $P_{l_1,l_s} = (\overline{Y}_{l_1} \cup \overline{Y}_{l_2} \cup \cdots \cup \overline{Y}_{l_s})$ a path if for each $i = 1, \ldots, s-1$, the regions $\overline{Y}_{l_i}$ and $\overline{Y}_{l_{i+1}}$ share a common $(d-1)$-dimensional manifold. Here, s is the length of the path P_{l_1,l_s}. Suppose there is a path P_{k,l^*} from Y_k to Y_{l^*} we denote path length

$$s_k = \{\#\text{ of } Y_l \text{ in } P_{k,l^*} = (\overline{Y}_k \cup \cdots \cup \overline{Y}_{l^*})\}$$

Let $X^* \subset \bar{Y}_{l^*}$ be a $(d-1)$ dimensional manifold, then for each $k = 1, 2, \ldots, n$ let $c_k^{X^*} > 0$ be the best constant so that

$$\left\| u - \bar{u}^{X^*} \right\|^2_{L^2(Y_k)} \leq (c_k^{X^*})^2 H^2 \|\nabla u\|^2_{L^2(P_{k,l^*})}, \tag{26}$$

for all $u \in H^1(P_{k,l^*})$. Note here we make a change of notation compared to [25], in that we replace $c_k^{X^*}$ with its square, similarly with C_P and related constants.

We now define the Poincaré inequality for a non-perforated domain. For any Lipschitz domain $Y \subset \mathbb{R}^d$ and for any $(d-1)$ dimensional manifold $X \subset \bar{Y}$, we denote $C_P(Y;X) > 0$ to be the best constant such that

$$\left\| u - \bar{u}^X \right\|^2_{L^2(Y)} \leq C_P^2(Y;X)\text{diam}(Y)^2 \|\nabla u\|^2_{L^2(Y)}, \tag{27}$$

for all $u \in H^1(Y)$. We have the following lemma relating the constants in (26) and (27).

Remark In our application we suppose this to be a simplicial domain such as a triangle, tetrahedron, or perhaps nonsimplicial, but regular, such as quadrilaterals, parallelepiped, or curved elements. The key here being that each simplex has a trivially bounded Poincaré constant.

Lemma 6.1 *Suppose P_{k,l^*} is a path as defined above of length s with $l_1 = k$ and $l_s = l^*$. We let $X_0 = X_1$ and $X_s = X^*$. Then, the constant from (26) can be bounded by the constants related to inequality (27)*

$$(c_k^{X^*})^2 \leq 4 \sum_{i=1}^{s} \frac{|Y_k|}{|Y_{l_i}|} \frac{\operatorname{diam}(Y_{l_i})^2}{H^2} \max(C_P^2(Y_{l_i}, X_{i-1}), C_P^2(Y_{l_i}, X_i)) \tag{28}$$

Proof We proceed as in [25], by using the standard telescoping argument

$$\left\| u - \bar{u}^{X^*} \right\|_{L^2(Y_k)} \leq \left\| u - \bar{u}^{X_1} \right\|_{L^2(Y_k)} + \sum_{i=2}^{s} \sqrt{|Y_k|} |\bar{u}^{X_{i-1}} - \bar{u}^{X_i}|,$$

and the use of (27) we have

$$\left\| u - \bar{u}^{X_1} \right\|^2_{L^2(Y_k)} \leq C_P^2(Y_k; X_1) \operatorname{diam}(Y_k)^2 \|\nabla u\|^2_{L^2(Y_k)}.$$

Fixing i we have for the second term

$$\begin{aligned} |\bar{u}^{X_{i-1}} - \bar{u}^{X_i}|^2 &\leq \frac{2}{|Y_{l_i}|} \left(\left\| u - \bar{u}^{X_{i-1}} \right\|^2_{L^2(Y_{l_i})} + \left\| u - \bar{u}^{X_i} \right\|^2_{L^2(Y_{l_i})} \right) \\ &\leq \frac{2}{|Y_{l_i}|} \left((C_P^2(Y_{l_i}; X_{i-1}) + C_P^2(Y_{l_i}; X_i)) \operatorname{diam}(Y_{l_i})^2 \|\nabla u\|^2_{L^2(Y_{l_i})} \right) \\ &\leq 4 \max(C_P^2(Y_{l_i}; X_{i-1}), C_P^2(Y_{l_i}; X_i)) \frac{\operatorname{diam}(Y_{l_i})^2}{|Y_{l_i}|} \|\nabla u\|^2_{L^2(Y_{l_i})}. \end{aligned}$$

A final application of the Cauchy inequality yields the desired result. □

We define $(C_P)^2 = \sum_{k=1}^{n} (c_k^{X^*})^2$ and we have the general full Poincaré inequality

$$\left\| u - \langle u \rangle_{\widetilde{\omega}} \right\|^2_{L^2(\widetilde{\omega}_x)} \leq \left\| u - \bar{u}^{X^*} \right\|^2_{L^2(\widetilde{\omega}_x)} \leq C_P^2 H^2 \|\nabla u\|^2_{L^2(\widetilde{\omega}_x)}, \tag{29}$$

recall here $\langle u \rangle_{\widetilde{\omega}} = \frac{1}{|\widetilde{\omega}_x|} \int_{\widetilde{\omega}_x} u dz$ is the optimal minimizing constant.

To obtain better bounds on C_P we must in turn obtain a systematic way to obtain bounds on $c_k^{X^*}$. To this end, we will use the following two technical lemmas. The first of which estimates the constant $C_P(K; F)$ for a simplex.

Lemma 6.2 *Let K be a simplex (or parallelepiped), and F one of its faces, then*

$$C_P^2(K; F) \leq \frac{7}{5}.$$

Proof See Appendix of [25].

We also state a common estimate for regular triangulation.

Lemma 6.3 *Let K a nondegenerate simplex and $\rho(K)$ the diameter of the largest sphere inscribed in $\bar{K}$, then*

$$|K| \geq \operatorname{diam}(K) \left(\frac{\rho(K)}{2} \right)^{d-1}.$$

Proof See Appendix of [25].

Let $\mathcal{Y} = \{Y_l\}_{l=1}^n$ be a conforming simplicial triangulation of $\widetilde{\omega}$ and we define the geometric parameters for $l = 0, \ldots, n$, $\eta_l = \text{diam}(Y_l)$, $\eta = \max(\eta_l)$, and $\eta_{min} = \min(\eta_l)$. We define the shape-regularity constant

$$C_{reg}^{\mathcal{Y}} = \max_{l=1}^{n} \left(\frac{\text{diam}(Y_l)}{\rho(Y_l)} \right).$$

We call a partition of $\widetilde{\omega}$ shape regular if there is a uniform bound for $C_{reg}^{\mathcal{Y}}$ and quasi-uniform if in addition to shape regular we have η/η_{min} uniformly bounded. With this type of a partition we are able to obtain a useful tool to estimate C_P.

Lemma 6.4 *Let $\mathcal{Y} = \{Y_l\}_{l=1}^n$ be a shape regular simplicial partition of $\widetilde{\omega}$, with X^* a facet of Y_{l^*}. We denote the path length for Y_k to Y_{l^*} by s_k. Then, we have the bound*

$$C_P^2 \leq \left(\frac{28}{5} \right) 2^{d+1} (C_{reg}^{\mathcal{Y}})^{d-1} \sum_{k=1}^{n} \frac{s_k |Y_k|}{H^2 \eta_{min}^{d-2}}. \tag{30}$$

Proof From Lemma 6.1 we have for a fixed k and path P_{k,l^*} of simplicial domains that

$$(c_k^{X^*})^2 \leq 4 \sum_{i=1}^{s_k} \frac{|Y_k|}{|Y_{l_i}|} \frac{\text{diam}(Y_{l_i})^2}{H^2} \max(C_P^2(Y_{l_i}, X_{i-1}), C_P^2(Y_{l_i}, X_i)).$$

For $i = 1, \ldots s_k$, using Lemma 6.2 we see, taking $K = Y_{l_i}$ and $F = X_{i-1}$ or $F = X_i$, that

$$\max(C_P^2(Y_{l_i}, X_{i-1}), C_P^2(Y_{l_i}, X_i)) \leq \frac{7}{5}.$$

From shape regularity and Lemma 6.3 we have

$$\frac{\text{diam}(Y_{l_i})^2}{|Y_{l_i}|} \leq 2^{d+1} (C_{reg}^{\mathcal{Y}})^{d-1} \eta_{l_i}^{2-d}.$$

Taking the minimum η_{l_i} we have

$$(c_k^{X^*})^2 \leq \left(\frac{28}{5} \right) \sum_{i=1}^{s_k} 2^{d+1} (C_{reg}^{\mathcal{Y}})^{d-1} \frac{|Y_k|}{H^2 \eta_{min}^{d-2}} \leq \left(\frac{28}{5} \right) 2^{d+1} (C_{reg}^{\mathcal{Y}})^{d-1} \frac{s_k |Y_k|}{H^2 \eta_{min}^{d-2}}.$$

Summing from $k = 1, \ldots n$ over the simplices we obtain the estimate. □

Remark As noted in [25], the above lemma can give "worst case" scenarios for estimates on Poincaré constants. To illustrate the usefulness of the above estimate (30) to obtain rough bounds we give an illustrative example. It can be easily seen that the estimate (30) will grow when the path lengths, s_k, are large. This can be especially bad in highly tortuous microstructures. We illuminate this by considering a two-dimensional filamented microstructure.

Suppose we take our domain to be $\omega = [0, H]^2$, and inside we have the solid microstructure, S_η, given by thin filamented structures. More precisely,

$$S_\eta = \bigcup_{j=0}^{N_\eta} \left(([4\eta j, 4\eta j + \eta] \times [0, H - \eta]) \cup ([4\eta j + 2\eta, 4\eta j + 3\eta] \times [\eta, H]) \right),$$

where $N_\eta \leq \left\lfloor \frac{H}{4\eta} \right\rfloor$. Note we take here the floor of $\frac{H}{4\eta}$ to ensure N_η is such that we have the right hand side boundary free of microstructure intersections. This is done since we will suppose that $X^* = \{H\} \times [0, H]$ and we wish this boundary to be a part of the domain $\widetilde{\omega}$ defined as

$$\widetilde{\omega} = \omega \backslash S_\eta.$$

Suppose we have a uniform shape regular square elements of $\widetilde{\omega}$ denoted again by $\mathcal{Y} = \{Y_l\}_{l=1}^n$. Moreover, we suppose that $|Y_k| \approx \eta^2$, for all $k = 1, \dots n$. We denote

$$s_{max} = \max_{k=1}^{n} s_k,$$

to be the maximal path length from Y_k to X^*. Then, (30) becomes

$$C_P^2 \lesssim C_{reg}^{\mathcal{Y}} \frac{n s_{max} \eta^2}{H^2}, \tag{31}$$

To estimate s_{max}, we take the simplex farthest from the right hand side boundary X^* denoted Y_1 to construct the longest path. Suppose that Y_1 is formed by $[0, \eta] \times [H - \eta, H]$. Then, we partition the rest of the filaments into square elements as seen in Figure 2, where the dots denote continuation. We can see that in each filament has path length is $O(\frac{H}{\eta})$ and there are $O(N_\eta) \approx O(\frac{H}{\eta})$ filaments. Hence $s_{max} \approx O((\frac{H}{\eta})^2)$, and in addition, we see also that $n \approx O((\frac{H}{\eta})^2)$ as this is the number of triangles in the partition of $\widetilde{\omega}$. We thus obtain the estimate for the Poincaré constant

$$C_P^2 \lesssim C_{reg}^{\mathcal{Y}} \left(\frac{H}{\eta}\right)^2. \tag{32}$$

Taking the maximum over the possible constants over the patches, and applying this estimate to Theorem

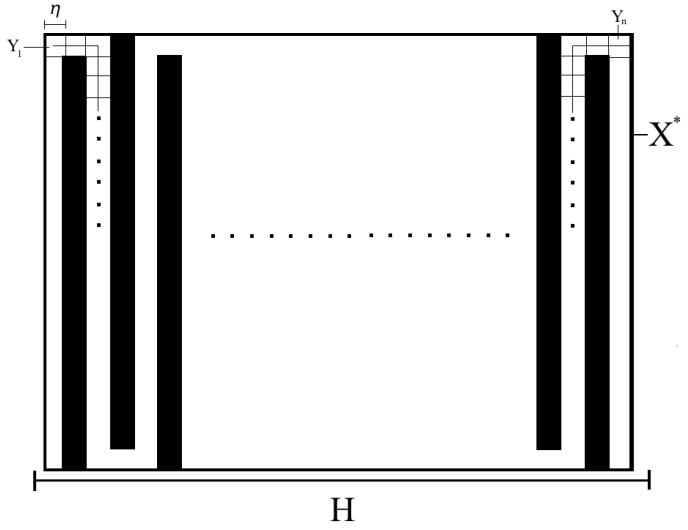

Figure 2: Filamented domain partitioned with squares and showing the longest paths.

5.3 we have

$$\left\|\nabla u - \nabla u_{H,m}^{ms}\right\|_{L^2(\widetilde{\Omega})} \lesssim \left(\left(C^{inv}\frac{H}{\eta}\right) H + m^{\frac{d}{2}} \left(\frac{H}{\eta}\right)^4 (C^{inv})^3 e^{-\left(\frac{\eta}{HC^{inv}}\right)^{\frac{3}{2}} m}\right) \|g\|_{L^2(\widetilde{\Omega})}. \tag{33}$$

Thus, it is possible to see how the closeness of the microstructure could theoretically effect the convergence estimate via the Poincaré. The constant in the exponential may also effect the decay with respect to patch extension. However, the above example is meant to represent a very poor scenario as different and more optimized partitions of the Figure 2 could clearly be constructed, thus improving the estimate. Again here from Appendix B the constant C^{inv} depends only volumetrically on the microstructure.

7 Numerical Examples

In this section we will present a two numerical examples. We apply our algorithm to (1) using our multiscale method and compare with standard $\mathbb{P}_1$ finite elements. By gridding around the perforations, we will implement the micro-structural features into the domain. We will do this for two relevant examples. The first being a periodic square domain with square particles, and the second an dumbbell-shaped domain containing the microstructure of the first experiment. We will demonstrate the validity of our estimates based on varying patch size (truncation of the localization) and by varying microstructure lengths η. When we vary the microstructure lengths we will also fix our truncation patch parameter k to be proportional to $\log(H)$.

We begin by describing the geometry of the domains. First, we take our unperforated domain to be $\Omega = [0,1]^2$ and define the unit cell to be $Y = [0,1]^2 \backslash [\frac{1}{4}, \frac{3}{4}]^2$. We define the perforated domain to be

$$\widetilde{\Omega}^\eta = \bigcup_{k \in \mathbb{Z}^2} (\eta(Y+k)) \cap \Omega, \tag{34}$$

where η is chosen so that the domain is periodically tessellated. This domain for $\eta = \frac{1}{8}$ can be seen in Figure 3.

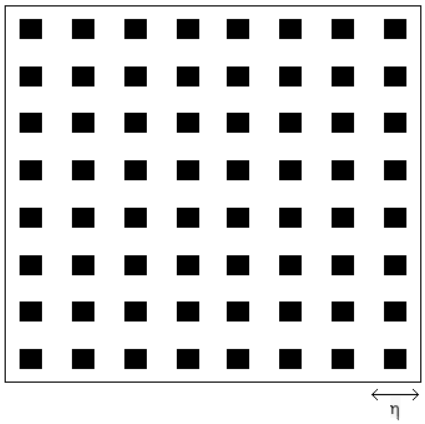

Figure 3: Square domain with periodic microstructure.

Since this geometry will clearly be in the same class as the uniform bound estimate (24), we choose our second geometry to be an dumbbell-shaped domain. As noted in [25], such a shaped domain has a theoretical bound $C_P^2 \leq 1 + \log(\text{diam}(\Omega))/\eta$. Here η is the separation of the narrowest part of the domain. More concretely, we let

$$\Omega^{H,\eta} = \Omega \backslash \left(\left([\frac{3}{8}, \frac{5}{8}] \times [0, \frac{1-\eta}{2}] \right) \cup \left([\frac{3}{8}, \frac{5}{8}] \times [\frac{1+\eta}{2}, 1] \right) \right).$$

In addition to the H structure we also take out some of the square perforations as in (34) for a fixed period of $\frac{1}{16}$. We define the following domain

$$\widetilde{\Omega}^{H,\eta} = \bigcup_{k \in \mathbb{Z}^2} \left(\frac{1}{16}(Y+k) \right) \cap \Omega^{H,\eta}, \tag{35}$$

this domain can be seen in Figure 4. Note here, the size of the perforations are fixed and the varying quantity is the size of the narrowest part of the domain in the middle strip.

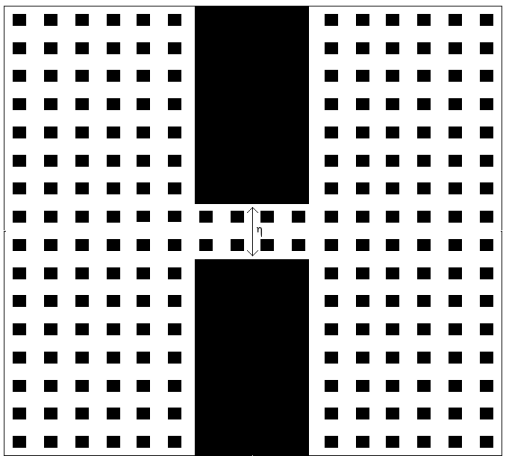

Figure 4: Dumbbell-shaped domain with periodic microstructure

To solve the problems in the porous domains, we will explicitly grid the perforations on the fine scale, not on the coarse scale. A penalization scheme could also be utilized to relax the restrictiveness of gridding the fine scale. Note, there is a fine scale h to solve the local problems and we take this value to be $h = 2^{-8}$. For all the following examples we will use the forcing

$$g(x_1, x_2) = \begin{cases} 1, x_2 \geq .5 \\ 0, x_2 < .5. \end{cases}$$

In addition to using the projective quasi-interpolation operator (6), we also present results from the Clément interpolation operator [22],

$$\widetilde{\mathcal{I}}_H u = \sum_{x \in \mathcal{N}_N} (\widetilde{\mathcal{I}}_H u)(x) \mathcal{R}\lambda_x, \tag{36}$$

where $(\widetilde{\mathcal{I}}_H u)(x) = \frac{\int_{\tilde{\Omega}} v\lambda_x dz}{\int_{\tilde{\Omega}} \lambda_x dz}$. Recall, we chose the projective quasi-interpolator only to simplify the proofs, and here we present numerical results to show that, in these cases, good results hold for the Clément interpolation operator also.

We present results for both media (34) and (35) while using both interpolation operators (6) and (36). We have two types of numerical tests. First, varying the microstructure parameter η while keeping the k-patch growth fixed to $\log(H)$. The idea here to see the effect of the error estimates from the possibly error degrading Poincaré constant. Second, we fix the microstructure length to the smallest value and vary the patch size to observe the rates of exponential convergence. All of these results are compared against an "overkill" fine-scale solution with $h = 2^{-8}$ in the H^1 norm.

The results from the geometry (34) are contained in Figure 5 and 6. In Figure 5, we use the projective interpolator (6) and in Figure 6 we use the Clément interpolator (36). Varying the microstructure, in the case period size η, while fixing the patch extension $k \approx \log(H)$ we plot the results for both interpolators in Figure 5a and Figure 6a. In both examples we see that the Poincaré constant does not effect the estimate negatively in agreement with (24). In Figure 5b and Figure 6b we fix the geometric parameter to the smallest value $\eta = 2^{-6}$ and vary the patch size parameter k. We note that projective quasi-interpolator performs better in this case at exponential convergence of the patch extensions.

The results from the geometry (35) are contained in Figure 7 and 8. In Figure 7, we use the projective interpolator (6) and in Figure 8 we use the Clément interpolator (36). Keeping the period fixed but varying η, the width of the thinnest part, and again fixing the patch extension $k \approx \log(H)$ we plot the results for both interpolators in Figure 7a and Figure 8a. In Figure 7b and Figure 8b we fix the geometric parameter

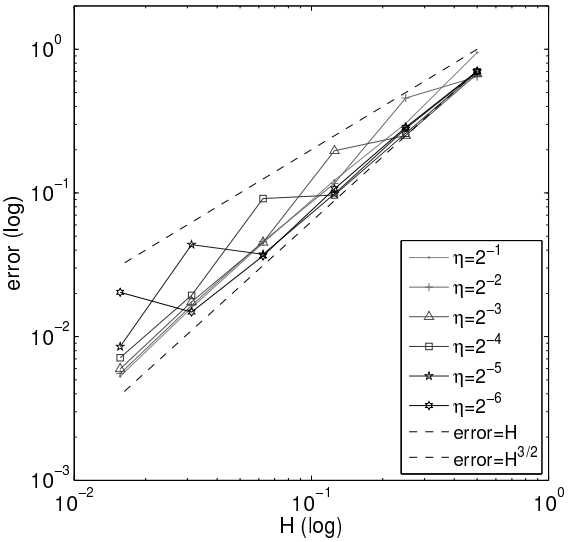

(a) Varying η for patch size $k \approx \log(H)$.

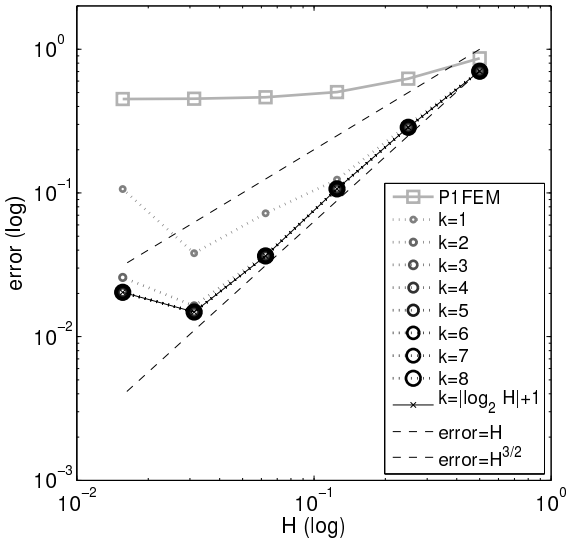

(b) Varying patch size k for $\eta = 2^{-6}$.

Figure 5: Results for example geometry in Figure 3, using projective quasi-interpolation (6).

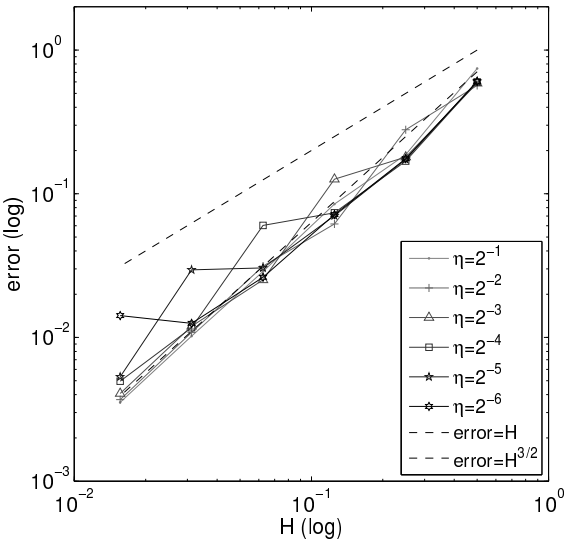

(a) Varying η for patch size $k \approx \log(H)$.

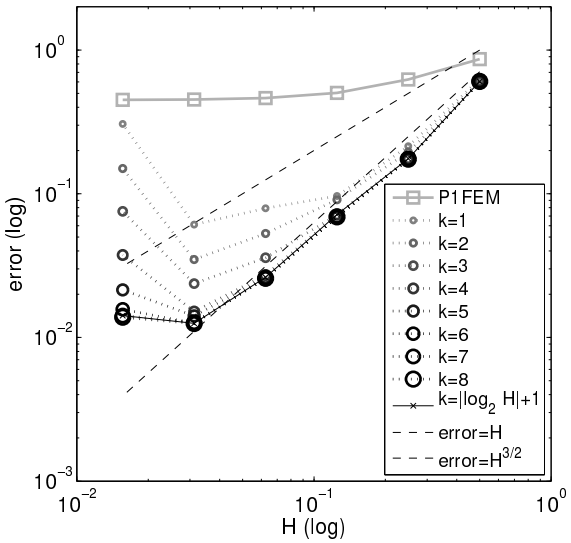

(b) Varying patch size k for $\eta = 2^{-6}$.

Figure 6: Results for example geometry in Figure 3, using Clément quasi-interpolation (36).

to the smallest value $\eta = 2^{-6}$ and vary the patch size parameter k. Again we see slightly better performance with respect to exponential convergence of the patch extensions for the projective quasi-interpolation.

8 Conclusion

In this work we developed a multiscale procedure to compute Laplacian problems with zero Neumann data in domains with complicated porous microstructure. We are were able to determine the error with respect to

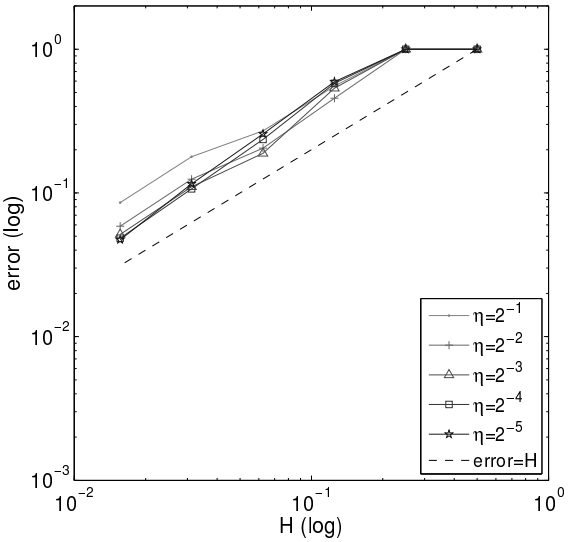

(a) Varying η for patch size $k \approx \log(H)$.

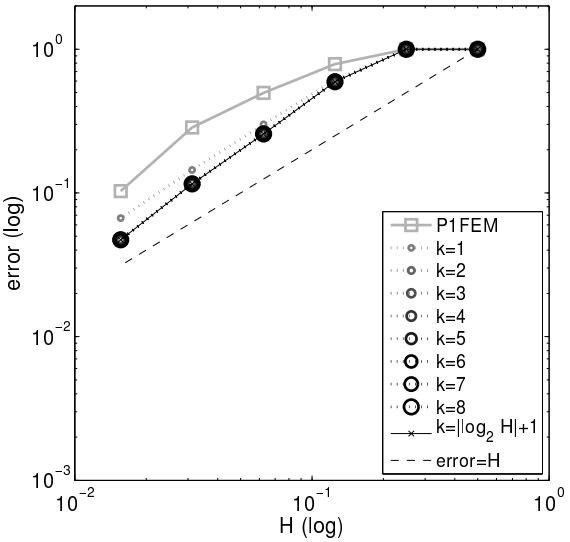

(b) Varying patch size k for $\eta = 2^{-6}$.

Figure 7: Results for example geometry in Figure 4, using projective quasi-interpolation (6).

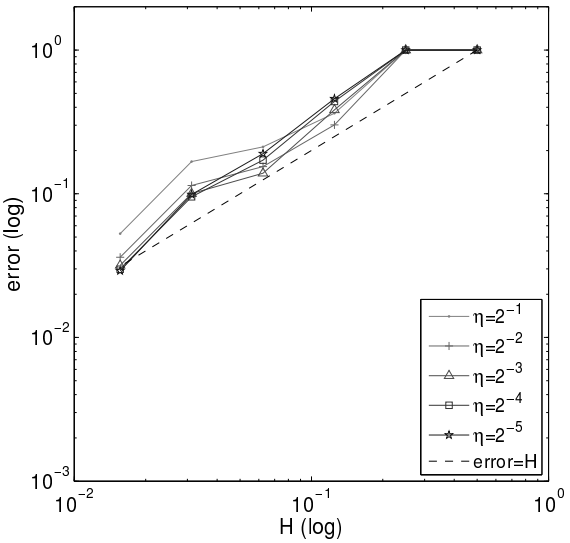

(a) Varying η for patch size $k \approx \log(H)$.

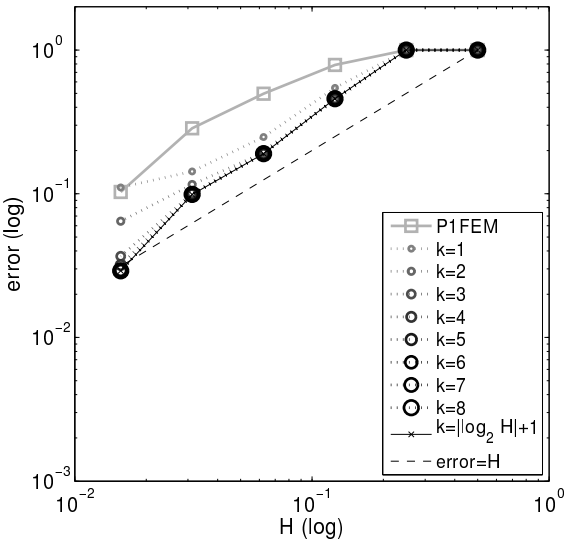

(b) Varying patch size k for $\eta = 2^{-6}$.

Figure 8: Results for example geometry in Figure 4, using Clément quasi-interpolation (36).

the ideal corrector and error due to truncation and localization of the multiscale correctors. As was noted, keeping track of Poincaré constants was critical in our analysis as they may contain information about the microstructure. We used a constructive procedure to estimate these constants and obtain bounds with respect to H and η. This procedure was demonstrated on two interesting examples. Finally, we implemented numerical tests to validate our theoretical estimates. We found our numerical experiments were in agreement with the theory and the quasi-interpolator based on local L^2 projections to perform slightly better than the Clément type.

9 Acknowledgements

We would like to acknowledge the anonymous reviewers for their helpful suggestions. Particularly, in the suggestion and proofs of the extension theorem and techniques for Poincaré constants. Their suggestions and helpful advice made this documents much stronger and we wish to acknowledge their contribution.

A Inverse Estimates on Perforated Domains

We will first need the inverse inequality in perforated domains. For $K \in \mathcal{T}_H$ and $p \in \mathbb{P}_1(K)$, the standard inverse inequality is given by

$$\|\nabla p\|_{L^2(K)} \lesssim H^{-1} \|p\|_{L^2(K)}, \tag{37}$$

where $H = \operatorname{diam}(K)$. However, for a perforated domain we shall be more careful and track the constants that may depend on the microstructure. Thus, we prove Lemma 3.1.

Proof of Lemma 3.1 Since for $p = c$, $c \in \mathbb{R}$, there is nothing to show, thus we suppose that $p \neq c$ and thus, $\nabla p \neq 0$. Since ∇p is a non-zero constant on K and by standard trace inequality (37)

$$\begin{aligned} \|\nabla p\|^2_{L^2(\tilde{K})} = \frac{|\tilde{K}|}{|K|} \|\nabla p\|^2_{L^2(K)} &= \frac{|\tilde{K}|}{|K|} \|\nabla (p - \langle p \rangle_K)\|^2_{L^2(K)} \\ &\lesssim \left(\frac{|\tilde{K}|}{|K|} \right) H^{-2} \|p - \langle p \rangle_K\|^2_{L^2(K)} . \end{aligned} \tag{38}$$

Since $p \neq c$, we can rewrite the right-hand-side as

$$\left(\frac{|\tilde{K}|}{|K|} \right) H^{-2} \|p - \langle p \rangle_K\|^2_{L^2(K)} = \left(\frac{|\tilde{K}|}{|K|} \right) H^{-2} \frac{\|p - \langle p \rangle_K\|^2_{L^2(K)}}{\|p - \langle p \rangle_{\tilde{K}}\|^2_{L^2(\tilde{K})}} \|p - \langle p \rangle_{\tilde{K}}\|^2_{L^2(\tilde{K})} . \tag{39}$$

Noting that since the average is the minimal constant, we have $\|p - \langle p \rangle_{\tilde{K}}\|_{L^2(\tilde{K})} \leq \|p\|_{L^2(\tilde{K})}$, and thus

$$\|\nabla p\|^2_{L^2(\tilde{K})} \lesssim \frac{|\tilde{K}|}{|K|} H^{-2} \left(\frac{\|p - \langle p \rangle_K\|^2_{L^2(K)}}{\|p - \langle p \rangle_{\tilde{K}}\|^2_{L^2(\tilde{K})}} \right) \|p\|^2_{L^2(\tilde{K})} . \tag{40}$$

It remains to bound the ratio of L^2 norms in K and $\tilde{K}$. First note that we may write in K

$$p - \langle p \rangle_K = \nabla p \cdot (x - \langle x \rangle_K).$$

The upper bound is clear, indeed we have that

$$\|p - \langle p \rangle_K\|^2_{L^2(K)} = |\nabla p|^2 \int_K |x - \langle x \rangle_K|^2 dx \lesssim |\nabla p|^2 H^2 |K|. \tag{41}$$

For the denominator bound, we introduce the notation for the zero set of $p - \langle p \rangle_{\tilde{K}}$ as

$$\mathcal{G} := \{x \in \mathbb{R}^d \,:\, p(x) - \langle p \rangle_{\tilde{K}} = 0\}.$$

Clearly, for a non-constant linear polynomial this is simply a hyperplane. We introduce the notation that $P_{\mathcal{G}} x$ be the orthogonal projection of x onto $\mathcal{G}$. It is clear that $\langle x \rangle_{\tilde{K}} \in \mathcal{G}$ and $\nabla p \perp \mathcal{G}$, thus we may write

$$p - \langle p \rangle_{\tilde{K}} = \nabla p \cdot (x - P_{\mathcal{G}} x).$$

For simplicity, and without loss of generality, we suppose that $\mathcal{G} = \{x \in \mathbb{R}^d : x_d = 0\}$, then $x - P_{\mathcal{G}}x = (0_{(d-1)}, x_d)$. Thus, since ∇p is constant

$$\|p - \langle p \rangle_{\tilde{K}}\|^2_{L^2(\tilde{K})} = \int_{\tilde{K}} |\nabla p \cdot (x - P_{\mathcal{G}}x)|^2 dx = \int_{\tilde{K}} |\nabla p \cdot (0, x_d)|^2 dx = \left|\frac{\partial p}{\partial x_d}\right|^2 \int_{\tilde{K}} x_d^2 dx.$$

We will now examine the quantity $\int_{\tilde{K}} x_d^2 dx$. We define the small δ-band around $\mathcal{G}$ to be $U_\delta = \mathbb{R}^{d-1} \times [-\frac{\delta}{2}, \frac{\delta}{2}]$. Then, choose $\delta > 0$, so that $|\tilde{K}| = |U_\delta \cap K|$. We have that

$$\int_{\tilde{K}} x_d^2 dx \geq \int_{U_\delta \cap K} x_d^2 dx \geq \int_{(U_\delta \cap K) \backslash U_{\delta/2}} x_d^2 dx \geq \frac{\delta^2}{4} |(U_\delta \cap K) \backslash U_{\delta/2}|.$$

Noting that $|(U_\delta \cap K) \backslash U_{\delta/2}| \approx |(U_\delta \cap K)| = |\tilde{K}|$ and $\delta \approx |\tilde{K}|/|\mathcal{G} \cap K| \gtrsim |\tilde{K}|/H^{d-1}$, we have

$$\frac{|\tilde{K}|^3}{H^{2d-2}} \lesssim \int_{\tilde{K}} x_d^2 dx.$$

Using this above estimate and returning to a general configuration, i.e. not necessarily on the line $x_d = 0$, we have the estimate

$$\frac{|\hat{K}^3|}{|K|} |\nabla p|^2 \lesssim \|p - \langle p \rangle_{\tilde{K}}\|^2_{L^2(\tilde{K})}. \tag{42}$$

Combining the lower bound (42), with the upper bound (41), we obtain the ratio

$$\frac{\|p - \langle p \rangle_K\|^2_{L^2(K)}}{\|p - \langle p \rangle_{\tilde{K}}\|^2_{L^2(\tilde{K})}} \lesssim \frac{|\nabla p|^2 H^2 |K|}{|\nabla p|^2 \frac{|\hat{K}^3|}{|K|}} \lesssim \left(\frac{|K|}{|\tilde{K}|}\right)^3.$$

Thus, using (40) and the above estimate of the ratio, we obtain

$$\|\nabla p\|^2_{L^2(\tilde{K})} \lesssim \left(\frac{|K|}{|\tilde{K}|}\right)^2 H^{-2} \|p\|^2_{L^2(\tilde{K})}, \tag{43}$$

and taking square roots yields the result. □

Thus, for many small (in the volumetric sense) perforations one would not expect too much contribution from the inverse inequality constant.

B Stability and Approximation Properties of Quasi-Interpolation

We now will prove the stability estimate used throughout for this projective quasi-interpolation operator (6). The proof of this lemma is based on that presented in [24].

Proof of Lemma 3.2 Note that we have easily from this definition taking $v_H = (\mathcal{P}_x u)$ and applying Cauchy-Schwarz thus, $\|\mathcal{P}_x u\|_{L^2(\widetilde{\omega}_x)} \leq \|u\|_{L^2(\widetilde{\omega}_x)}$. We use $u - \langle u \rangle_{\widetilde{\omega}_x}$, here again $\langle u \rangle_{\widetilde{\omega}_x} = \frac{1}{|\widetilde{\omega}_x|} \int_{\widetilde{\omega}_x} u dz$, the fact that the L^2 projection of a constant is itself, and the fact that $(1 - \mathcal{P}_x)$ is also a projection we obtain

$$\|u - \mathcal{P}_x u\|_{L^2(\widetilde{\omega}_x)} \leq \left\|u - \langle u \rangle_{\widetilde{\omega}_x}\right\|_{L^2(\widetilde{\omega}_x)} \leq H C_P \|\nabla u\|_{L^2(\widetilde{\omega}_x)}. \tag{44}$$

Here, we used the inequality (8) to obtain the gradient bound. To obtain the derivative bound note that by a use of the inverse inequality from Lemma 3.1 and (8) we have

$$\begin{aligned}
\|\nabla(u - \mathcal{P}_x u)\|_{L^2(\widetilde{\omega}_x)} &= \left\|\nabla(u - \mathcal{P}_x(u - \langle u \rangle_{\widetilde{\omega}_x})\right\|_{L^2(\widetilde{\omega}_x)} \\
&\leq \|\nabla u\|_{L^2(\widetilde{\omega}_x)} + \left\|\nabla \mathcal{P}_x(u - \langle u \rangle_{\widetilde{\omega}_x})\right\|_{L^2(\widetilde{\omega}_x)} \\
&\leq \|\nabla u\|_{L^2(\widetilde{\omega}_x)} + C^{inv} H^{-1} \left\|\mathcal{P}_x(u - \langle u \rangle_{\widetilde{\omega}_x})\right\|_{L^2(\widetilde{\omega}_x)} \\
&\leq (1 + C^{inv} C_P) \|\nabla u\|_{L^2(\widetilde{\omega}_x)}
\end{aligned} \tag{45}$$

This is merely the H^1 stability of the L^2 projection c.f. [3] and references therein.

We suppose that the basis functions form a partition of unity, that is $\sum_{y\in\mathcal{N}_H}\lambda_y = 1$, as we will deal with the elements adjacent to the boundary with a slight technical difference. We first treat the elements that do not meet the boundary. If the elements meet the boundary the Friedrichs' inequality can be utilized and we will briefly discuss this later. Thus, we have for the L^2 norm

$$\begin{aligned}
\left\|u-\widetilde{\mathcal{I}}_H u\right\|_{L^2(\widetilde{\omega}_x)} &= \left\|u-\sum_{y\in\mathcal{N}_H}(\mathcal{P}_y u)(y)\lambda_y\right\|_{L^2(\widetilde{\omega}_x)}\\
&= \left\|\sum_{y\in\mathcal{N}_H}(u-(\mathcal{P}_y u)(y))\lambda_y\right\|_{L^2(\widetilde{\omega}_x)}\\
&\leq \sum_{y\in\mathcal{N}_H(\widetilde{\omega}_x)}\left\|u-(\mathcal{P}_y u)(y)\right\|_{L^2(\widetilde{\omega}_x)}\\
&\leq \sum_{y\in\mathcal{N}_H(\widetilde{\omega}_x)}\left\|u-\mathcal{P}_y u\right\|_{L^2(\widetilde{\omega}_x)} + \sum_{y\in\mathcal{N}_H(\widetilde{\omega}_x)}\left\|\mathcal{P}_y u-(\mathcal{P}_y u)(y)\right\|_{L^2(\widetilde{\omega}_x)}, \qquad (46)
\end{aligned}$$

where $\mathcal{N}_H(\widetilde{\omega}_x)$ denotes the coarse nodes in the patch $\widetilde{\omega}_x$. We can easily estimate the first term by using (44), taking a closer look at the second term, again using the partition of unity property, we have for $x'\in\mathcal{N}_H(\widetilde{\omega}_x)$ that

$$\begin{aligned}
\left\|\mathcal{P}_y u-(\mathcal{P}_y u)(y)\right\|_{L^2(\widetilde{\omega}_x)} &= \left\|\sum_{x'\in\mathcal{N}_H(\widetilde{\omega}_x)}\left((\mathcal{P}_y u)(x')-(\mathcal{P}_y u)(y)\right)\lambda_{x'}\right\|_{L^2(\widetilde{\omega}_x)}\\
&\leq \sum_{x'\in\mathcal{N}_H(\widetilde{\omega}_x)}\left\|(\mathcal{P}_y u)(x')-(\mathcal{P}_y u)(y)\right\|_{L^2(\widetilde{\omega}_x)}\\
&\leq \sum_{x'\in\mathcal{N}_H(\widetilde{\omega}_x)}|\widetilde{\omega}_x|^{\frac{1}{2}}|(\mathcal{P}_y u)(x')-(\mathcal{P}_y u)(y)|\\
&\lesssim \sum_{x'\in\mathcal{N}_H(\widetilde{\omega}_x)}|\widetilde{\omega}_x|^{\frac{1}{2}}H\left\|\nabla\mathcal{P}_y u\right\|_{L^\infty(\widetilde{\omega}_x)}\\
&\lesssim \sum_{x'\in\mathcal{N}_H(\widetilde{\omega}_x)}H\left\|\nabla\mathcal{P}_y u\right\|_{L^2(\widetilde{\omega}_x)}
\end{aligned}$$

Returning to (46), and using inequalities (44) and (45) we have

$$\begin{aligned}
\left\|u-\widetilde{\mathcal{I}}_H u\right\|_{L^2(\widetilde{\omega}_x)} &\leq \sum_{y\in\mathcal{N}_H(\widetilde{\omega}_x)}\left\|u-\mathcal{P}_y u\right\|_{L^2(\widetilde{\omega}_x)} + \left\|\mathcal{P}_y u-(\mathcal{P}_y u)(y)\right\|_{L^2(\widetilde{\omega}_x)}\\
&\lesssim \sum_{y\in\mathcal{N}_H(\widetilde{\omega}_{x,1})}HC_P\left\|\nabla u\right\|_{L^2(\widetilde{\omega}_{x,1})} + \sum_{x'\in\mathcal{N}_H(\widetilde{\omega}_x)}H\left\|\nabla\mathcal{P}_y u\right\|_{L^2(\widetilde{\omega}_x)}\\
&\lesssim \sum_{y\in\mathcal{N}_H(\widetilde{\omega}_{x,1})}HC_P\left\|\nabla u\right\|_{L^2(\widetilde{\omega}_{x,1})} + \sum_{x'\in\mathcal{N}_H(\widetilde{\omega}_x)}C^{inv}\left\|(\mathcal{P}_y(u-\langle u\rangle_{\widetilde{\omega}_x}))\right\|_{L^2(\widetilde{\omega}_x)}\\
&\lesssim (1+C^{inv})C_P H\left\|\nabla u\right\|_{L^2(\widetilde{\omega}_{x,1})}. \qquad (47)
\end{aligned}$$

Using the estimate (45), and a similar argument as above for the L^2 estimate [24], we will obtain the derivative estimate

$$\left\|\nabla(u-\widetilde{\mathcal{I}}_H u)\right\|_{L^2(\widetilde{\omega}_x)} \lesssim \left(1+(1+C^{inv})C_P\right)\left\|\nabla u\right\|_{L^2(\widetilde{\omega}_{x,1})}. \qquad (48)$$

We proceed similarly as with the L^2 estimate for the H^1 and have

$$\begin{aligned}
\left\|\nabla(u-\widetilde{\mathcal{I}}_H u)\right\|_{L^2(\widetilde{\omega}_x)} &= \left\|\nabla\left(u-\sum_{y\in\mathcal{N}_H}(\mathcal{P}_y u)(y)\lambda_y\right)\right\|_{L^2(\widetilde{\omega}_x)} \\
&= \left\|\nabla\sum_{y\in\mathcal{N}_H}(u-(\mathcal{P}_y u)(y))\lambda_y\right\|_{L^2(\widetilde{\omega}_x)} \\
&\leq \sum_{y\in\mathcal{N}_H(\widetilde{\omega}_x)}\left\|\nabla\left(u-(\mathcal{P}_y u)(y)\right)\lambda_y)\right\|_{L^2(\widetilde{\omega}_x)} \\
&\leq \sum_{y\in\mathcal{N}_H(\widetilde{\omega}_x)}\left\|(u-(\mathcal{P}_y u)(y))\nabla\lambda_y)\right\|_{L^2(\widetilde{\omega}_x)} + \left\|\nabla\left(u-(\mathcal{P}_y u)(y)\right)\lambda_y)\right\|_{L^2(\widetilde{\omega}_x)} \\
&\lesssim \sum_{y\in\mathcal{N}_H(\widetilde{\omega}_x)} H^{-1}\left\|(u-(\mathcal{P}_y u)(y)))\right\|_{L^2(\widetilde{\omega}_x)} + \left\|\nabla\left(u-(\mathcal{P}_y u)(y)\right)\right\|_{L^2(\widetilde{\omega}_x)}, \qquad (49)
\end{aligned}$$

here we used that that $|\nabla\lambda_y|\lesssim H^{-1}$ and $|\lambda_y|\lesssim 1$. Clearly we can estimate the first term by (47), however, we will lose an order H. To estimate the second term we note since $(\mathcal{P}_y u)(y)$ is constant, we have

$$\sum_{y\in\mathcal{N}_H(\widetilde{\omega}_x)}\left\|\nabla\left(u-(\mathcal{P}_y u)(y)\right)\right\|_{L^2(\widetilde{\omega}_x)} \lesssim \|\nabla u\|_{L^2(\widetilde{\omega}_{x,1})}. \qquad (50)$$

To handle an element on the boundary we use the Friedrich's inequality which has a constant that is benign with respect to the perforations. Suppose we have $\widetilde{\omega}_x$ that meets $\partial\Omega$. Then, $u=\widetilde{\mathcal{I}}_H(u)=0$ on $\partial\Omega$, and so

$$\left\|u-\widetilde{\mathcal{I}}_H(u)\right\|_{L^2(\widetilde{\omega}_x)} \leq C_{FP}H\left\|\nabla(u-\widetilde{\mathcal{I}}_H(u))\right\|_{L^2(\widetilde{\omega}_x)} \leq C^{inv}C_{FP}H\|\nabla u\|_{L^2(\widetilde{\omega}_{x,1})}, \qquad (51)$$

and so we have trivially $C^{inv}C_{FP}\lesssim C^{inv}C_P$.

To see the $\widetilde{\mathcal{I}}_H$ is a projection note for $\mathcal{P}_x$, the local patch L^2 projection, acting on $\mathcal{R}\lambda_x$ is a projection, and moreover is identity. By definition we have

$$\int_{\widetilde{\omega}_x}(\mathcal{P}_x^2\lambda_x)v_H dz = \int_{\widetilde{\omega}_x}\lambda_x v_H dz \text{ for all } v_H\in V_H|_{\omega_x} \qquad (52)$$

and thus it is trivial to see $\mathcal{P}_x^2\lambda_x=\mathcal{P}_x\lambda_x=\lambda_x$ on $\widetilde{\omega}_x$ for all $x\in\mathcal{N}_H$. Thus,

$$\widetilde{\mathcal{I}}_H(\mathcal{R}\lambda_x)=\sum_{x'\in\mathcal{N}_H}(\mathcal{P}_{x'}(\mathcal{R}\lambda_{x'}))(x)\mathcal{R}\lambda_x=\sum_{x'\in\mathcal{N}_H}(\mathcal{R}\lambda_{x'})(x')\mathcal{R}\lambda_x=\mathcal{R}\lambda_x,$$

and so $\widetilde{\mathcal{I}}_H^2(\mathcal{R}\lambda_x)=\widetilde{\mathcal{I}}_H(\mathcal{R}\lambda_x)=\mathcal{R}\lambda_x$, and so by linearity

$$\widetilde{\mathcal{I}}_H^2(u)=\widetilde{\mathcal{I}}_H\left(\sum_{x\in\mathcal{N}_H}(\mathcal{P}_x u)(x)\mathcal{R}\lambda_x\right)=\sum_{x\in\mathcal{N}_H}(\mathcal{P}_x u)(x)\widetilde{\mathcal{I}}_H(\mathcal{R}\lambda_x)=\sum_{x\in\mathcal{N}_H}(\mathcal{P}_x u)(x)\mathcal{R}\lambda_x.$$

From here we see that $\widetilde{\mathcal{I}}_H^2=\widetilde{\mathcal{I}}_H$. □

C Auxiliary Lemmas

Now we will prove and state the auxiliary lemmas used to prove estimate (18). These proofs are largely based on the works [13, 22] and references therein. However, here we must carefully track the occurrence of Poincaré constants.

First, we begin with the quasi-incusion property. For $x, x' \in \mathcal{N}_H$ and $l, k \in \mathbb{N}$ and $m = 0, 1, \cdots$, with $k \geq l \geq 2$ we have if

$$\widetilde{\omega}_{x',m+1} \cap (\widetilde{\omega}_{x,k} \backslash \widetilde{\omega}_{x,l}) \neq \emptyset, \text{ then } \widetilde{\omega}_{x',1} \subset (\widetilde{\omega}_{x,k+m+1} \backslash \widetilde{\omega}_{x,l-m-1}.) \tag{53}$$

We will use the cutoff functions defined in [13]. For $x \in \mathcal{N}_H$ and $k > l \in \mathbb{N}$, let $\eta_x^{k,l} : \widetilde{\Omega} \to [0,1]$ be a continuous weakly differentiable functions so that

$$\left(\eta_x^{k,l}\right)|_{\widetilde{\omega}_{x,k-l}} = 0, \tag{54a}$$

$$\left(\eta_x^{k,l}\right)|_{\widetilde{\Omega} \backslash \widetilde{\omega}_{x,k}} = 1, \tag{54b}$$

$$\forall T \in \mathcal{T}_H, \left\|\nabla \eta_x^{k,l}\right\|_{L^\infty(T)} \leq C_{co} \frac{1}{lH}, \tag{54c}$$

where C_{co} is only dependent on the shape regularity of the mesh $\mathcal{T}_H$. We may choose here the cutoff function as in [22] where we choose a function, $\eta_x^{k,l}$, in the space of $\mathbb{P}_1$ Lagrange finite elements over $\mathcal{T}_H$ such that

$$\begin{aligned}
&\eta_x^{k,l}(y) = 0 \text{ for all } y \in \mathcal{N}_H \cap \omega_{x,k-l}, \\
&\eta_x^{k,l}(y) = 1 \text{ for all } y \in \mathcal{N}_H \cap (\Omega \backslash \omega_{x,k}), \\
&\eta_x^{k,l}(y) = \frac{j}{l} \text{ for all } y \in \mathcal{N}_H \cap \omega_{x,k-l+j}, j = 0, 1, \ldots, l,
\end{aligned}$$

then, restrict the above function to the perforated domain without relabeling.

Unlike in [13], we are using a quasi-interpolation that is also a projection. This simplifies the proofs since there is no need to construct an approximate projection. Here we will need the following simplified quasi-invariance of the fine-scale space under multiplication by cutoff functions. We write this estimate in the following lemma.

Lemma C.1 *Let $k > l \in \mathbb{N}$ and $x \in \mathcal{N}_H$. Suppose that $w \in \widetilde{V}^f$, then we have the estimate*

$$\left\|\nabla \widetilde{\mathcal{I}}_H(\eta_x^{k,l} w)\right\|_{L^2(\widetilde{\Omega})} \leq C_1 l^{-1} \|\nabla w\|_{L^2(\widetilde{\omega}_{x,k+2} \backslash \widetilde{\omega}_{x,k-l-2})}, \tag{55}$$

here $C_1 = (C_{lip}^2 C_{\mathcal{I}_H} + C_{\mathcal{I}_H}^3)^{1/2} \lesssim (C^{inv} C_P)^{3/2}$.

Proof Fixing x and k, we denote the average as $\langle \eta_x^{k,l} \rangle_{\widetilde{\omega}_{x',1}} = \frac{1}{|\widetilde{\omega}_{x',1}|} \int_{\widetilde{\omega}_{x',1}} \eta_x^{k,l} dz$. We estimate on a single patch $\widetilde{\omega}_x$, using the fact that $\widetilde{\mathcal{I}}_H(w) = 0$ and the estimate (10) we have

$$\begin{aligned}
&\left\|\nabla \widetilde{\mathcal{I}}_H(\eta_x^{k,l} w)\right\|_{L^2(\widetilde{\omega}_{x'})} = \left\|\nabla \widetilde{\mathcal{I}}_H((\eta_x^{k,l} - \langle \eta_x^{k,l} \rangle_{\widetilde{\omega}_{x',1}}) w)\right\|_{L^2(\widetilde{\omega}_{x'})} \\
&\leq C_{\mathcal{I}_H} \left\|\nabla((\eta_x^{k,l} - \langle \eta_x^{k,l} \rangle_{\widetilde{\omega}_{x',1}}) w)\right\|_{L^2(\widetilde{\omega}_{x',1})} \\
&\leq C_{\mathcal{I}_H} \left(\left\|(\eta_x^{k,l} - \langle \eta_x^{k,l} \rangle_{\widetilde{\omega}_{x',1}}) \nabla w\right\|_{L^2(\widetilde{\omega}_{x',1})} + \left\|\nabla \eta_x^{k,l} (w - \widetilde{\mathcal{I}}_H(w))\right\|_{L^2(\widetilde{\omega}_{x',1})} \right).
\end{aligned}$$

Summing over all $x \in \mathcal{N}_H$, using the quasi-inclusion property (53), and the above calculation yields

$$\begin{aligned}
\left\|\nabla \widetilde{\mathcal{I}}_H(\eta_x^{k,l} w)\right\|_{L^2(\widetilde{\Omega})}^2 &\leq \sum_{x' \in \mathcal{N}_H} \left\|\nabla \widetilde{\mathcal{I}}_H(\eta_x^{k,l} w)\right\|_{L^2(\widetilde{\omega}_{x'})}^2 \\
&\leq C_{\mathcal{I}_H} \sum_{\widetilde{\omega}_{x'} \subset \widetilde{\omega}_{x,k+2} \backslash \widetilde{\omega}_{x,k-l-2}} \left\|\nabla((\eta_x^{k,l} - \langle \eta_x^{k,l} \rangle_{\widetilde{\omega}_{x',1}}) w)\right\|_{L^2(\widetilde{\omega}_{x',1})}^2 \\
&\leq C_{\mathcal{I}_H} \sum_{\widetilde{\omega}_{x'} \subset \widetilde{\omega}_{x,k+2} \backslash \widetilde{\omega}_{x,k-l-2}} \left\|(\eta_x^{k,l} - \langle \eta_x^{k,l} \rangle_{\widetilde{\omega}_{x',1}}) \nabla w\right\|_{L^2(\widetilde{\omega}_{x',1})}^2 \\
&+ C_{\mathcal{I}_H} \sum_{\widetilde{\omega}_{x'} \subset \widetilde{\omega}_{x,k+2} \backslash \widetilde{\omega}_{x,k-l-2}} \left\|\nabla \eta_x^{k,l} (w - \widetilde{\mathcal{I}}_H(w))\right\|_{L^2(\widetilde{\omega}_{x',1})}^2.
\end{aligned}$$

Noting that $\nabla\eta_x^{k,l} \neq 0$ only in $\widetilde{\omega}_{x,k}\backslash\widetilde{\omega}_{x,k-l}$ and $(\eta_x^{k,l} - \langle\eta_x^{k,l}\rangle_{\widetilde{\omega}_{x',1}}) \neq 0$ only if $\widetilde{\omega}_{x',k}$ intersects $\widetilde{\omega}_{x,k}\backslash\widetilde{\omega}_{x,k-l}$ hence we obtain the tighter estimate

$$\begin{aligned}\left\|\nabla\widetilde{\mathcal{I}}_H(\eta_x^{k,l}w)\right\|^2_{L^2(\widetilde{\Omega})} &\leq C_{\mathcal{I}_H}\sum_{\widetilde{\omega}_{x'}\subset\widetilde{\omega}_{x,k+1}\backslash\widetilde{\omega}_{x,k-l-1}}\left\|(\eta_x^{k,l} - \langle\eta_x^{k,l}\rangle_{\widetilde{\omega}_{x',1}})\nabla w\right\|^2_{L^2(\widetilde{\omega}_{x',1})}\\ &+ C_{\mathcal{I}_H}\sum_{\widetilde{\omega}_{x'}\subset\widetilde{\omega}_{x,k+1}\backslash\widetilde{\omega}_{x,k-l-1}}\left\|\nabla\eta_x^{k,l}(w - \widetilde{\mathcal{I}}_H(w))\right\|^2_{L^2(\widetilde{\omega}_{x',1})}.\end{aligned}$$

Using the fact that $\eta_x^{k,l}$ is taken to be $\mathbb{P}_1$ and thus constant on each element, we have the bound

$$\begin{aligned}\left\|\eta_x^{k,l} - \langle\eta_x^{k,l}\rangle_{\widetilde{\omega}_{x',1}}\right\|_{L^\infty(\widetilde{\omega}_{x',1})} &\lesssim |\widetilde{\omega}_{x',1}|^{-1/2}C^{inv}\left\|\eta_x^{k,l} - \langle\eta_x^{k,l}\rangle_{\widetilde{\omega}_{x',1}}\right\|_{L^2(\widetilde{\omega}_{x',1})}\\ &\lesssim |\widetilde{\omega}_{x',1}|^{-1/2}C^{inv}C_PH\left\|\nabla\eta_x^{k,l}\right\|_{L^2(\widetilde{\omega}_{x',1})}\\ &\lesssim |\widetilde{\omega}_{x',1}|^{-1/2}C^{inv}C_PH\sum_{\tilde{K}\in\widetilde{\omega}_{x',1}}\left\|\nabla\eta_x^{k,l}\right\|_{L^2(\tilde{K})}\\ &\lesssim |\widetilde{\omega}_{x',1}|^{-1/2}C^{inv}C_PH\sum_{\tilde{K}\in\widetilde{\omega}_{x',1}}|\tilde{K}|^{1/2}\left\|\nabla\eta_x^{k,l}\right\|_{L^\infty(\tilde{K})}\\ &\lesssim C^{inv}C_PH\left\|\nabla\eta_x^{k,l}\right\|_{L^\infty(\widetilde{\omega}_{x',1})},\end{aligned} \tag{56}$$

where we will denote in this section $C_{lip} = C^{inv}C_P$. Using the above relation on the first term and (10) on the second we obtain

$$\begin{aligned}\left\|\nabla\widetilde{\mathcal{I}}_H(\eta_x^{k,l}w)\right\|^2_{L^2(\widetilde{\Omega})} &\leq C_{lip}^2C_{\mathcal{I}_H}H^2\left\|\nabla\eta_x^{k,l}\right\|^2_{L^\infty(\widetilde{\Omega})}\|\nabla w\|^2_{L^2(\widetilde{\omega}_{x,k+1}\backslash\widetilde{\omega}_{x,k-l-1})}\\ &+ C^3_{\mathcal{I}_H}H^2\left\|\nabla\eta_x^{k,l}\right\|^2_{L^\infty(\widetilde{\Omega})}\|\nabla w\|^2_{L^2(\widetilde{\omega}_{x,k+1}\backslash\widetilde{\omega}_{x,k-l-1})}.\end{aligned}$$

Finally, taking another layer on the outside and inside of the annulus patch we arrive at

$$\left\|\nabla\widetilde{\mathcal{I}}_H(\eta_x^{k,l}w)\right\|^2_{L^2(\widetilde{\Omega})} \leq l^{-2}(C_{lip}^2C_{\mathcal{I}_H} + C^3_{\mathcal{I}_H})\|\nabla w\|^2_{L^2(\widetilde{\omega}_{x,k+2}\backslash\widetilde{\omega}_{x,k-l-2})},$$

here $C_1^2 = C_{lip}^2C_{\mathcal{I}_H} + C^3_{\mathcal{I}_H}$. Note that trivially $C_{lip} \lesssim C^{inv}C_P$, thus, $C_1 \lesssim (C^{inv}C_P)^{3/2}$. □

We now will demonstrate the decay of the fine-scale space in the next lemma.

Lemma C.2 *Fix some $x \in \mathcal{N}_H$ and $F \in (\widetilde{V}^f)'$ the dual of $\widetilde{V}^f$ satisfying $F(w) = 0$ for all $w \in \widetilde{V}^f(\widetilde{\Omega}\backslash\widetilde{\omega}_{x,1})$. Then, for $u \in \widetilde{V}^F$ the solution of*

$$\int_{\widetilde{\Omega}}\nabla u\nabla w dz = F(w) \text{ for all } w \in \widetilde{V}^f. \tag{57}$$

Then, there exists a constant $\theta \in (0,1)$ such that for $k \in \mathbb{N}$ we have

$$\|\nabla u\|_{L^2(\widetilde{\Omega}\backslash\widetilde{\omega}_{x,k})} \leq \theta^k\|\nabla u\|_{L^2(\widetilde{\Omega})}. \tag{58}$$

We have $\theta = e^{-\frac{1}{\lceil C_2e\rceil+2}} \in (0,1)$, here $C_2 \lesssim (C_1 + C_{\mathcal{I}_H}) \lesssim (C^{inv}C_P)^{3/2}$

Proof Letting $\eta_x^{k,l}$ be the cut-off function as in the previous lemma for $l < k-3$. Let $\tilde{u} = \eta_x^{k,l}u - \widetilde{\mathcal{I}}_H(\eta_x^{k,l}u) \in \widetilde{V}^f(\widetilde{\Omega}\backslash\widetilde{\omega}_{x,k-l-2})$, and note that from Lemma C.1 we have

$$\left\|\nabla(\eta_x^{k,l}u - \tilde{u})\right\|_{L^2(\widetilde{\Omega})} = \left\|\nabla\widetilde{\mathcal{I}}_H(\eta_x^{k,l}u)\right\|_{L^2(\widetilde{\Omega})} \leq C_1l^{-1}\|\nabla u\|_{L^2(\widetilde{\omega}_{x,k+2}\backslash\widetilde{\omega}_{x,k-l-2})}, \tag{59}$$

from this estimate and the properties of F we have

$$\int_{\widetilde{\Omega}\setminus\widetilde{\omega}_{x,k-l-2}} \nabla u \nabla \tilde{u} dz = \int_{\widetilde{\Omega}} \nabla u \nabla \tilde{u} dz = F(\tilde{u}) = 0. \tag{60}$$

We have via Caccioppoli type argument that

$$\|\nabla u\|^2_{L^2(\widetilde{\Omega}\setminus\widetilde{\omega}_{x,k})} \leq \int_{\widetilde{\Omega}\setminus\widetilde{\omega}_{x,k-l-2}} \eta_x^{k,l} |\nabla u|^2 dz \tag{61}$$

$$\leq \int_{\widetilde{\Omega}\setminus\widetilde{\omega}_{x,k-l-2}} \nabla u \left(\nabla(\eta_x^{k,l} u) - u\nabla\eta_x^{k,l}\right) dz. \tag{62}$$

Using the fact that $\widetilde{\mathcal{I}}_H(u) = 0$, estimate (59), and the relation (60) we have

$$\begin{aligned}
\|\nabla u\|^2_{L^2(\widetilde{\Omega}\setminus\widetilde{\omega}_{x,k})} &\leq \int_{\widetilde{\Omega}\setminus\widetilde{\omega}_{x,k-l-2}} \nabla u(\nabla(\eta_x^{k,l}u) - \tilde{u}) dz \\
&\quad - \int_{\widetilde{\Omega}\setminus\widetilde{\omega}_{x,k-l-2}} \nabla u(u - \widetilde{\mathcal{I}}_H(u))\nabla\eta_x^{k,l} dz \\
&\lesssim C_1 l^{-1} \|\nabla u\|^2_{L^2(\widetilde{\Omega}\setminus\widetilde{\omega}_{x,k-l-2})} \\
&\quad + (lH)^{-1} \|\nabla u\|_{L^2(\widetilde{\Omega}\setminus\widetilde{\omega}_{x,k-l-2})} \left\|u - \widetilde{\mathcal{I}}_H(u)\right\|_{L^2(\widetilde{\Omega}\setminus\widetilde{\omega}_{x,k-l-2})} \\
&\lesssim l^{-1} C_2 \|\nabla u\|^2_{L^2(\widetilde{\Omega}\setminus\widetilde{\omega}_{x,k-l-2})}.
\end{aligned}$$

On the last term we used the projection estimate (10) and here $C_2 \lesssim (C_1 + C_{\mathcal{I}_H})$. Note here that this C is the benign constant from the estimate of $\nabla\eta_x^{k,j}$. Taking $l = \lceil C_2 e \rceil$ and successive applications of the above estimate yields

$$\begin{aligned}
\|\nabla u\|^2_{L^2(\widetilde{\Omega}\setminus\widetilde{\omega}_{x,k})} &\leq e^{-1} \|\nabla u\|^2_{L^2(\widetilde{\Omega}\setminus\widetilde{\omega}_{x,k-l-2})} \\
&\leq e^{-\lfloor \frac{k-1}{l+2} \rfloor} \|\nabla u\|^2_{L^2(\widetilde{\Omega}\setminus\widetilde{\omega}_{x,1})} \leq e^{-\lfloor \frac{k}{l+2} \rfloor} \|\nabla u\|^2_{L^2(\widetilde{\Omega})}.
\end{aligned}$$

Finally, taking $\theta = e^{-\frac{1}{\lceil C_2 e \rceil + 2}}$ yields the result. □

We now are ready to state our result on the error introduced from localization. The heart of this argument is to estimate the error between the truncated corrector Q_k constructed, after summing over x from (15) and the ideal corrector when k is large enough so that we obtain $Q_{\widetilde{\Omega}}$.

Lemma C.3 *Let $u_H \in \widetilde{V}_H$, let Q_m be constructed from* (15)*, and $Q_{\widetilde{\Omega}}$ defined to be the "ideal" corrector without truncation, then*

$$\left\|\nabla(Q_{\widetilde{\Omega}}(u_H) - Q_m(u_H))\right\|_{L^2(\widetilde{\Omega})} \leq m^{\frac{d}{2}} C_4 \theta^m \left\|\nabla Q_{\widetilde{\Omega}}(u_H)\right\|_{L^2(\widetilde{\Omega})}, \tag{63}$$

with $C_3 \lesssim (1 + C_1 + C_{\mathcal{I}_H}) \lesssim (C^{inv} C_P)^{3/2}$ and $C_4 = C_3(1 + C_1^2)^{\frac{1}{2}} \lesssim (C^{inv} C_P)^3$.

Proof Recall that $Q_m(u_H) = \sum_{x\in\mathcal{N}_H} Q_{x,m}(u_H)$ with

$$\int_{\widetilde{\omega}_{x,m}} \nabla Q_{x,m}(u_H) \nabla w dz = \int_{\widetilde{\omega}_x} \hat{\lambda}_x \nabla u_H \nabla w, dz \text{ for all } w \in \widetilde{V}^f(\widetilde{\omega}_{x,m}). \tag{64}$$

For all $x \in \mathcal{N}_H$, and letting $F_x(w) := \int_{\widetilde{\Omega}} \hat{\lambda}_x \nabla u_H \nabla w dz$. Note that for $w \in \widetilde{V}^f(\widetilde{\Omega}\setminus\widetilde{\omega}_x)$, we have $F_x(w) = 0$. Let $x \in \mathcal{N}_H$ and choose a $x' \in \mathcal{N}_H$ such that $\widetilde{\omega}_{x'} \cap \widetilde{\omega}_x \neq \emptyset$. We have $\widetilde{\omega}_x \subset \widetilde{\omega}_{x',1}$ and so $\widetilde{V}^f(\widetilde{\Omega}\setminus\widetilde{\omega}_{x',1}) \subset \widetilde{V}^f(\widetilde{\Omega}\setminus\widetilde{\omega}_x)$. Thus, F_x satisfies the conditions of Lemma C.2.

Choosing $k \geq m$, we have that $\widetilde{\omega}_{x',k} \subset \widetilde{\omega}_{x,m}$. We denote $v = Q_{\widetilde{\Omega}}(u_H) - Q_m(u_H)) \in \widetilde{V}^f$, subsequently $\widetilde{\mathcal{I}}_H(v) = 0$. Taking the cut-off function $\eta_{x'}^{k,1}$ we have

$$\|\nabla v\|^2_{L^2(\widetilde{\Omega})} = \sum_{x\in\mathcal{N}_H} \int_{\widetilde{\Omega}} \nabla(Q_{x,\widetilde{\Omega}}(u_H) - Q_{x,m}(u_H))\nabla(v(1-\eta_{x'}^{k,1}))dz \tag{65}$$

$$+ \sum_{x\in\mathcal{N}_H} \int_{\widetilde{\Omega}} \nabla(Q_{x,\widetilde{\Omega}}(u_H) - Q_{x,m}(u_H))\nabla(v\eta_{x'}^{k,1})dz. \tag{66}$$

Estimating the right hand side of (65) for each x we have

$$\begin{aligned}
&\int_{\widetilde{\Omega}} \nabla(Q_{x,\widetilde{\Omega}}(u_H) - Q_{x,m}(u_H))\nabla(v(1-\eta_{x'}^{k,1}))dz\\
&\leq \left\|\nabla(Q_{x,\widetilde{\Omega}}(u_H) - Q_{x,m}(u_H))\right\|_{L^2(\widetilde{\Omega})} \left\|\nabla(v(1-\eta_{x'}^{k,1}))\right\|_{L^2(\widetilde{\omega}_{x',k})}\\
&\leq \left\|\nabla(Q_{x,\widetilde{\Omega}}(u_H) - Q_{x,m}(u_H))\right\|_{L^2(\widetilde{\Omega})} \left(\|\nabla v\|_{L^2(\widetilde{\omega}_{x',k})} + \left\|v\nabla(1-\eta_{x'}^{k,1}))\right\|_{L^2(\widetilde{\omega}_{x',k}\setminus\widetilde{\omega}_{x',k-1})}\right)\\
&\leq \left\|\nabla(Q_{x,\widetilde{\Omega}}(u_H) - Q_{x,m}(u_H))\right\|_{L^2(\widetilde{\Omega})} \left(\|\nabla v\|_{L^2(\widetilde{\omega}_{x',k})} + CH^{-1}\left\|v - \widetilde{\mathcal{I}}_H(v)\right\|_{L^2(\widetilde{\omega}_{x',k}\setminus\widetilde{\omega}_{x',k-1})}\right)\\
&\leq \left\|\nabla(Q_{x,\widetilde{\Omega}}(u_H) - Q_{x,m}(u_H))\right\|_{L^2(\widetilde{\Omega})} (1 + CC_{\mathcal{I}_H}) \|\nabla v\|_{L^2(\widetilde{\omega}_{x',k+1})}.
\end{aligned}$$

As in the proof of Lemma C.2, $\tilde{v} = \eta_{x'}^{k,1}v - \widetilde{\mathcal{I}}_H(\eta_{x'}^{k,1}v) \in \widetilde{V}^f(\widetilde{\Omega}\setminus\widetilde{\omega}_{x',k-3})$. Letting m be large enough so that $k \geq 4$, then $\tilde{v} \in \widetilde{V}^f(\widetilde{\Omega}\setminus\widetilde{\omega}_x)$ and so we have

$$\int_{\widetilde{\Omega}} \nabla(Q_{x,\widetilde{\Omega}}(u_H) - Q_{x,m}(u_H))\nabla\tilde{v}dz = 0. \tag{67}$$

We have now the estimate for (66) for $x \in \mathcal{N}_H$ using the above identity and (59)

$$\begin{aligned}
&\int_{\widetilde{\Omega}} \nabla(Q_{x,\widetilde{\Omega}}(u_H) - Q_{x,m}(u_H))\nabla(v\eta_{x'}^{k,1} - \tilde{v})dz\\
&\leq \left\|\nabla(Q_{x,\widetilde{\Omega}}(u_H) - Q_{x,m}(u_H))\right\|_{L^2(\widetilde{\Omega})} \left\|\nabla(v\eta_{x'}^{k,1} - \tilde{v})\right\|_{L^2(\widetilde{\Omega})}\\
&\leq \left\|\nabla(Q_{x,\widetilde{\Omega}}(u_H) - Q_{x,m}(u_H))\right\|_{L^2(\widetilde{\Omega})} C_1\|\nabla v\|_{L^2(\widetilde{\omega}_{x',k+2})}
\end{aligned}$$

Combing the estimates for (65) and (66) we obtain

$$\begin{aligned}
\|\nabla v\|^2_{L^2(\widetilde{\Omega})} &\leq \sum_{x\in\mathcal{N}_H} \left\|\nabla(Q_{x,\widetilde{\Omega}}(u_H) - Q_{x,m}(u_H))\right\|_{L^2(\widetilde{\Omega})} (1 + CC_{\mathcal{I}_H}) \|\nabla v\|_{L^2(\widetilde{\omega}_{x',k+1})}\\
&+ \sum_{x\in\mathcal{N}_H} \left\|\nabla(Q_{x,\widetilde{\Omega}}(u_H) - Q_{x,m}(u_H))\right\|_{L^2(\widetilde{\Omega})} C_1\|\nabla v\|_{L^2(\widetilde{\omega}_{x',k+2})}\\
&\leq \sum_{x\in\mathcal{N}_H} \left\|\nabla(Q_{x,\widetilde{\Omega}}(u_H) - Q_{x,m}(u_H))\right\|_{L^2(\widetilde{\Omega})} (1 + C_1 + CC_{\mathcal{I}_H})\|\nabla v\|_{L^2(\widetilde{\omega}_{x',k+2})}\\
&\leq k^{\frac{d}{2}} C_3 \left(\sum_{x\in\mathcal{N}_H} \left\|\nabla(Q_{x,\widetilde{\Omega}}(u_H) - Q_{x,m}(u_H))\right\|^2_{L^2(\widetilde{\Omega})}\right)^{\frac{1}{2}} \|\nabla v\|_{L^2(\widetilde{\Omega})},
\end{aligned} \tag{68}$$

supposing the $\#\{x \in \mathcal{N}_H | \widetilde{\omega}_x \subset \widetilde{\omega}_{x',k+2}\} \leq k^{\frac{d}{2}}$, as is guaranteed by quasi-uniformity of the coarse grid. Here we have $C_3 = (1 + C_1 + CC_{\mathcal{I}_H})$. To estimate $\left\|\nabla(Q_{x,\widetilde{\Omega}}(u_H) - Q_{x,m}(u_H))\right\|_{L^2(\widetilde{\Omega})}$ we use the Galerkin

orthogonality of the local problem, that is

$$\left\|\nabla(Q_{x,\widetilde{\Omega}}(u_H)-Q_{x,m}(u_H))\right\|_{L^2(\widetilde{\Omega})}\leq \inf_{q\in\widetilde{V}^f(\widetilde{\omega}_{x',k})}\left\|\nabla(Q_{x,\widetilde{\Omega}}(u_H)-q)\right\|_{L^2(\widetilde{\Omega})}. \tag{69}$$

Taking $q_x=(1-\eta_{x'}^{k,1})Q_{x,\widetilde{\Omega}}(u_H)-\widetilde{\mathcal{I}}_H((1-\eta_{x'}^{k,1})Q_{x,\widetilde{\Omega}}(u_H))\in\widetilde{V}^f(\widetilde{\omega}_{x',k})$, we have

$$\begin{aligned}\left\|\nabla(Q_{x,\widetilde{\Omega}}(u_H)-Q_{x,m}(u_H))\right\|^2_{L^2(\widetilde{\Omega})}&\leq\left\|\nabla(\eta_{x'}^{k,1}Q_{x,\widetilde{\Omega}}(u_H)-\widetilde{\mathcal{I}}_H((1-\eta_{x'}^{k,1})Q_{x,\widetilde{\Omega}}(u_H)))\right\|^2_{L^2(\widetilde{\Omega})}\\&\leq\left\|\nabla Q_{x,\widetilde{\Omega}}(u_H)\right\|^2_{L^2(\widetilde{\Omega}\setminus\widetilde{\omega}_{x',k-2})}+\left\|\nabla(\widetilde{\mathcal{I}}_H((1-\eta_{x'}^{k,1})Q_{x,\widetilde{\Omega}}(u_H)))\right\|^2_{L^2(\widetilde{\Omega})}.\end{aligned}$$

Using Lemma C.1 and Lemma C.2 on the second term we arrive at

$$\begin{aligned}\left\|\nabla(Q_{x,\widetilde{\Omega}}(u_H)-Q_{x,m}(u_H))\right\|^2_{L^2(\widetilde{\Omega})}&\leq\left\|\nabla Q_{x,\widetilde{\Omega}}(u_H)\right\|^2_{L^2(\widetilde{\Omega}\setminus\widetilde{\omega}_{x',k-2})}+C_1^2\left\|\nabla Q_{x,\widetilde{\Omega}}(u_H))\right\|^2_{L^2(\widetilde{\omega}_{x',k+2}\setminus\widetilde{\omega}_{x',k-3})}\\&\leq(1+C_1^2)\left\|\nabla Q_{x,\widetilde{\Omega}}(u_H)\right\|^2_{L^2(\widetilde{\Omega}\setminus\widetilde{\omega}_{x',k-3})}\\&\leq(1+C_1^2)\theta^{2(k-3)}\left\|\nabla Q_{x,\widetilde{\Omega}}(u_H)\right\|^2_{L^2(\widetilde{\Omega})}\\&\leq(1+C_1^2)\theta^{2m}\left\|\nabla Q_{x,\widetilde{\Omega}}(u_H)\right\|^2_{L^2(\widetilde{\Omega})}.\end{aligned}$$

Combining this estimate into (68) we arrive at the final estimate that

$$\begin{aligned}\|\nabla v\|_{L^2(\widetilde{\Omega})}&\leq k^{\frac{d}{2}}C_3\left(\sum_{x\in\mathcal{N}_H}\left\|\nabla(Q_{x,\widetilde{\Omega}}(u_H)-Q_{x,m}(u_H))\right\|^2_{L^2(\widetilde{\Omega})}\right)^{\frac{1}{2}}\\&\leq k^{\frac{d}{2}}C_3\left(\sum_{x\in\mathcal{N}_H}(1+C_1^2)\theta^{2m}\left\|\nabla Q_{x,\widetilde{\Omega}}(u_H)\right\|^2_{L^2(\widetilde{\Omega})}\right)^{\frac{1}{2}}\\&\leq m^{\frac{d}{2}}C_4\theta^m\left\|\nabla Q_{\widetilde{\Omega}}(u_H)\right\|_{L^2(\widetilde{\Omega})}.\end{aligned}$$

Here we used $Q_{\widetilde{\Omega}}=\sum_{x\in\mathcal{N}_H}Q_{x,\widetilde{\Omega}}$ and denoted $C_4=C_3(1+C_1^2)^{\frac{1}{2}}$. □

References

[1] A. Abdulle and P. Henning. Localized orthogonal decomposition method for the wave equation with a continuum of scales. *ArXiv e-print 1406.6325*, 2014.

[2] Assyr Abdulle, Weinan E, Björn Engquist, and Eric Vanden-Eijnden. The heterogeneous multiscale method. *Acta Numer.*, 21:1–87, 2012.

[3] R. E. Bank and H. Yserentant. On the H1-stability of the L2-projection onto finite element spaces. *Numerische Mathematik*, 126(2):361–381, 2014.

[4] John W. Barrett and Charles M. Elliott. A finite-element method for solving elliptic equations with Neumann data on a curved boundary using unfitted meshes. *IMA J. Numer. Anal.*, 4(3):309–325, 1984.

[5] Peter Bastian and Christian Engwer. An unfitted finite element method using discontinuous Galerkin. *Internat. J. Numer. Methods Engrg.*, 79(12):1557–1576, 2009.

[6] Claude Le Bris, Frédéric Legoll, and Alexei Lozinski. An MsFEM type approach for perforated domains. *Multiscale Model. Simul.*, 12(3):1046–1077, 2014.

[7] I.V. Burenkov. Extension of functions with preservation of sobolev semi norm. *Trudy Mat. Inst. Steklov.*, 172:71–85, 1985.

[8] G. A. Chechkin, A. L. Piatniski, and A. S. Shamev. *Homogenization: Methods and Applications*, volume 234 of *Translations of Mathematical Monographs*. American Mathematical Society, Providence, RI, 2007.

[9] Y. Efendiev and T. Hou. *Multiscale Finite Element Methods: Theory and Applications*, volume 4 of *Surveys and Tutorials in the Applied Mathematical Sciences*. Springer, New York, NY, 2009.

[10] Stefano Giani and Paul Houston. *hp*-adaptive composite discontinuous Galerkin methods for elliptic problems on complicated domains. *Numer. Methods Partial Differential Equations*, 30(4):1342–1367, 2014.

[11] W. Hackbusch and S. A. Sauter. Composite finite elements for the approximation of PDEs on domains with complicated micro-structures. *Numer. Math.*, 75(4):447–472, 1997.

[12] P. Henning, A. Målqvist, and D. Peterseim. Two-level discretization techniques for ground state computations of bose-einstein condensates. *SIAM J. Numer. Anal.*, 52(4):1525–1550, 2014.

[13] P. Henning, P. Morgenstern, and D. Peterseim. Multiscale Partition of Unity. In M. Griebel and M. A. Schweitzer, editors, *Meshfree Methods for Partial Differential Equations VII*, volume 100 of *Lecture Notes in Computational Science and Engineering*. Springer, 2014. Also available as INS Preprint No. 1315.

[14] Patrick Henning, Axel Målqvist, and Daniel Peterseim. A localized orthogonal decomposition method for semi-linear elliptic problems. *ESAIM: Mathematical Modelling and Numerical Analysis*, eFirst, 12 2013.

[15] Patrick Henning and Mario Ohlberger. The heterogeneous multiscale finite element method for elliptic homogenization problems in perforated domains. *Numer. Math*, pages 601–629.

[16] Patrick Henning and Daniel Peterseim. Oversampling for the Multiscale Finite Element Method. *Multiscale Model. Simul.*, 11(4):1149–1175, 2013.

[17] T. J. R. Hughes and G. Sangalli. Variational multiscale analysis: the fine-scale Green's function, projection, optimization, localization, and stabilized methods. *SIAM J. Numer. Anal.*, 45(2):539–557, 2007.

[18] Thomas J. R. Hughes, Gonzalo R. Feijóo, Luca Mazzei, and Jean-Baptiste Quincy. The variational multiscale method—a paradigm for computational mechanics. *Comput. Methods Appl. Mech. Engrg.*, 166(1-2):3–24, 1998.

[19] Florian Liehr, Tobias Preusser, Martin Rumpf, Stefan Sauter, and Lars Ole Schwen. Composite finite elements for 3D image based computing. *Comput. Vis. Sci.*, 12(4):171–188, 2009.

[20] Axel Målqvist. Multiscale methods for elliptic problems. *Multiscale Model. Simul.*, 9(3):1064–1086, 2011.

[21] Axel Målqvist and Daniel Peterseim. Computation of eigenvalues by numerical upscaling. *Numerische Mathematik*, pages 1–25, 2014.

[22] Axel Målqvist and Daniel Peterseim. Localization of elliptic multiscale problems. *Math. Comp.*, 83(290):2583–2603, 2014.

[23] E. Marusic-Paloka and A. Mikelic. An error estimate for correctors in the homogenization of the Stokes and Navier-Stokes equations in a porous medium. *Bollettino U.M.I*, 7:661–671, 1996.

[24] M. Ohlberger. Numerik Partieller Differentialgleichungen 1. *Unpublished Notes*, 2008.

[25] Clemens Pechstein and Robert Scheichl. Weighted poincaré inequalities. *IMA Journal of Numerical Analysis*, 33(2):652–686, 2013.

[26] D. Peterseim. Variational multiscale stabilization and the exponential decay of fine-scale correctors. *ArXiv e-prints*, May 2015. Also available as INS Preprint No. 1509.

[27] D. Peterseim and R. Scheichl. Robust numerical upscaling of elliptic multiscale problems at high-contrast. *(in preparation)*, 2014.

[28] E. Sanchez-Palencia. *Non-Homogeneous Media and Vibration Theory*, volume 127 of *Lecture Notes in Physics*. Springer-Verlag, Berlin, 1980.

[29] S.A. Sauter. On extension theorems for domains having small geometric details. *Technical Report 96-03, University of Kiel*, 1996.

[30] S.A. Sauter and R. Warnke. Extension operators and approximation on domains containing small geometric details. *East West Journal of Numerical Mathematics*, 7:61–77, 1999.

[31] E. M. Stein. *Singular integrals and differentiability properties of functions*, volume 2. Princeton university press, 1970.